

000 001 002 003 004 005 006 007 008 009 010 011 012 013 014 015 016 017 018 019 020 021 022 023 024 025 026 027 028 029 030 031 032 033 034 035 036 037 038 039 040 041 042 043 044 045 046 047 048 049 050 051 052 053 OCEANGYM: A BENCHMARK ENVIRONMENT FOR UNDERWATER EMBODIED AGENTS

Anonymous authors

Paper under double-blind review

ABSTRACT

We introduce OCEANGYM, the first comprehensive benchmark for ocean underwater embodied agents, designed to advance AI in one of the most demanding real-world environments. Unlike terrestrial or aerial domains, underwater settings present extreme perceptual and decision-making challenges, including low visibility, dynamic ocean currents, making effective agent deployment exceptionally difficult. OCEANGYM encompasses eight realistic task domains and a unified agent framework driven by Multi-modal Large Language Models (MLLMs), which integrates perception, memory, and sequential decision-making. Agents are required to comprehend optical and sonar data, autonomously explore complex environments, and accomplish long-horizon objectives under these harsh conditions. Extensive experiments reveal substantial gaps between state-of-the-art MLLM-driven agents and human experts, highlighting the persistent difficulty of perception, planning, and adaptability in ocean underwater environments. By providing a high-fidelity, rigorously designed platform, OCEANGYM establishes a testbed for developing robust embodied AI and transferring these capabilities to real-world autonomous ocean underwater vehicles, marking a decisive step toward intelligent agents capable of operating in one of Earth’s last unexplored frontiers.

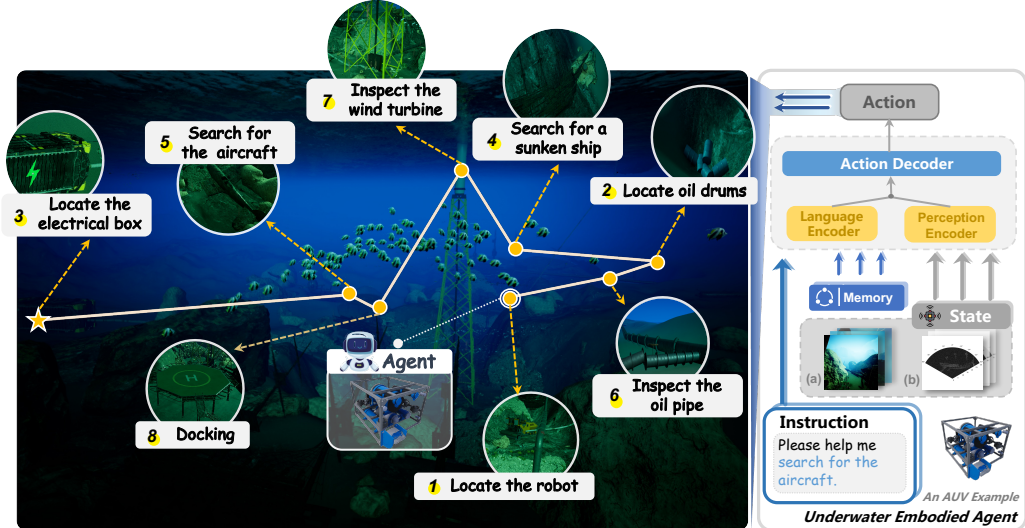


Figure 1: **Illustration of OCEANGYM.** The OCEANGYM benchmark introduces a unified **agent framework** across **8 real-world underwater scenarios**. The agent interprets language instruction, fuses optical and sonar imagery, and controls Autonomous Underwater Vehicles (AUVs).

1 INTRODUCTION

As Richard S. Sutton famously noted, we are entering an “era of experience” (Silver & Sutton, 2025). Embodied agents equipped with language models (Zhao et al., 2023; OpenAI, 2024) are emerging as a central paradigm for intelligent systems, as they accumulate and leverage experience through continuous interaction to close the perception-decision-action loop in physical or simulated environments (Gupta et al., 2021; Ding et al., 2024; Liu et al., 2025). Unlike static decision or generative

models, these agents must integrate rich multimodal sensory streams and execute continuous-control policies to achieve long-horizon objectives. This necessitates a unified treatment of perceptual representation, planning, online inference, and sequential policy optimization (Fung et al., 2025). Significant progress has been demonstrated across diverse domains, including robotic manipulators (Anderson et al., 2018; Caesar et al., 2020; Vasudevan et al., 2021; Gao et al., 2024), drones (Wang et al., 2024a; Lee et al., 2025; Gao et al., 2025b), and autonomous vehicles (Ma et al., 2025b).

In contrast, *underwater*¹ embodied agents remain largely unexplored despite their critical scientific and engineering importance (Visbeck, 2018; Kelly et al., 2022; Zheng et al., 2023; Li et al., 2024b; Gao et al., 2025a). Deploying embodied agents in marine environments offers unique opportunities for ocean exploration, offshore resource development, environmental monitoring, and subsea rescue operations. These tasks impose stringent requirements on the robustness and reliability of autonomous platforms, making the development of agents capable of functioning under real marine conditions a key bridge between simulated research and practical deployment (Ma et al., 2025a).

Challenges. Underwater embodied agents face distinct challenges that set them apart from overland and aerial systems. *Perceptually*, poor visibility and low-light conditions, combined with the inherent limitations of optical sensors, compel reliance on sonar, inertial measurements, and other sparse modalities (Li et al., 2024c; Aubard et al., 2025). These heterogeneous and noisy observations complicate sensor fusion and perception. *Environmentally*, deep-sea and offshore settings are largely unexplored, with unstable localization, absent prior knowledge, and dynamic currents. The lack of prior knowledge prevents effective environmental modeling, requiring agents to reason under circumstances of extreme partial observability and uncertainty (Sariman et al., 2025). Together, these factors constrain the development of underwater agents, leaving their capabilities in early stages.

Building OceanGym. To address these challenges, we introduce OCEANGYM, an open environment benchmark for underwater embodied agents. OCEANGYM constructs a comprehensive marine environment spanning approximately 800m × 800m (length × width), with dynamically adjustable depth to simulate varying lighting conditions. The platform incorporates eight distinct task domains designed to reflect real-world operational requirements. Additionally, it provides a multimodal LLM-based agent framework that integrates perception, memory, and action decision-making capabilities for controlling Autonomous Underwater Vehicles (AUVs). The benchmark unifies perception and decision-making in simulated underwater scenarios, where agents must infer target states from contextual cues or multi-view sensor data and execute complex behaviors such as search, inspection, and docking. **By simulating these environments, OCEANGYM enables systematic evaluation of language models' capabilities in underwater embodied settings and offers a pathway for transferring learned skills to real-world underwater vehicles through the generation of synthetic data, reinforcement learning guided by environmental feedback, and iterative improvement of agent capabilities through various algorithmic approaches.** We discuss the limitations of OCEANGYM in §3.3.

Benchmark Results and Insights. Extensive experiments on OCEANGYM reveal that Multi-modal Large Language Models (MLLMs) exhibit significant gaps compared to human experts, particularly under low-visibility conditions (decision-making success rate drops to 14.8%). Agents frequently struggle to interpret sonar data accurately, distinguish objects in complex environments, and maintain consistent deviation strategies over extended missions. Limitations also arise in memory retention and adaptability when objects are occluded or conditions change dynamically. These findings highlight persistent challenges for embodied AI in underwater environments and underscore the need for continued research in robust perception, reasoning, and control under extreme uncertainty.

2 OCEANGYM

OCEANGYM is a high-fidelity embodied underwater environment that simulates a realistic ocean setting with diverse scenes. As illustrated in Figure 2, OCEANGYM establishes a robust benchmark for evaluating autonomous agents through a series of challenging tasks, encompassing various perception analyses and decision-making navigation. OCEANGYM facilitates these evaluations by enabling MLLM-driven agents with multi-modal perception and parameterized action spaces.

¹Underwater refers to the ocean environment throughout this work and is not further specified.

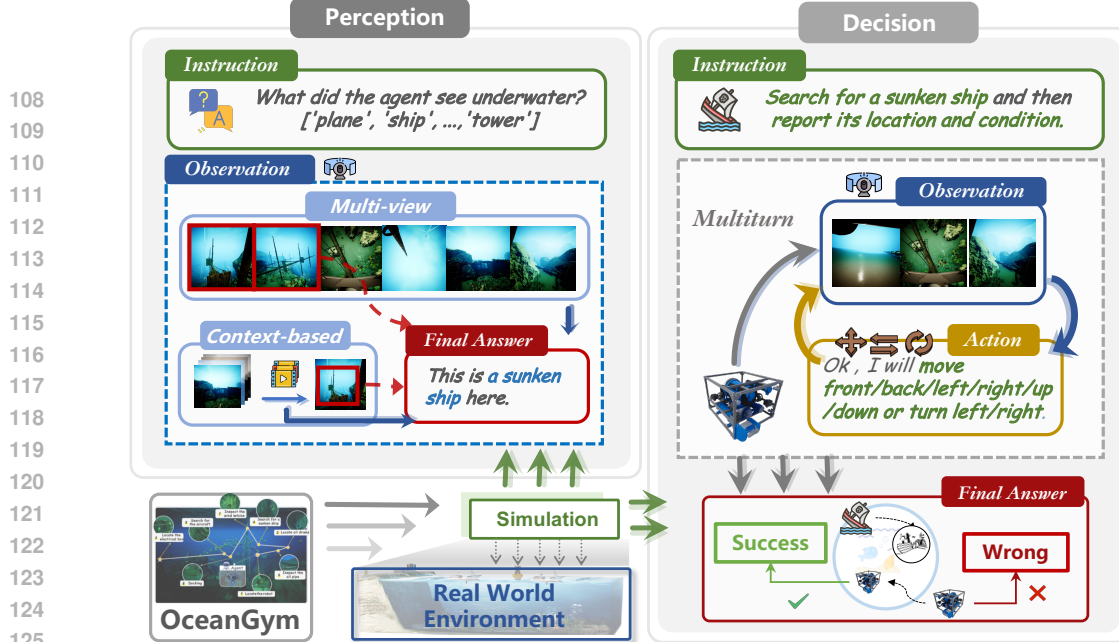


Figure 2: **OCEANGYM Tasks.** OCEANGYM comprises **Perception Tasks** (divided into **Multi-view Perception** and **Context-based Perception** settings) and **Decision Tasks** for evaluating embodied agents.

2.1 OCEANGYM ENVIRONMENT

We develop OCEANGYM atop Unreal Engine (UE) 5.3 (Epic Games, 2025), providing a comprehensive set of underwater environments, including both natural terrains and engineered structures. The environment features several semantic regions such as open water, seabed plains, underwater cliffs, pipeline networks, wreckage sites, and energy infrastructure zones. Each region is modeled with realistic physical and geometric properties, incorporating elements like oil pipelines, chemical waste barrels, submerged shipwrecks, electrical equipment, wind turbine foundations, and aircraft debris (more details in Appendix A.4). These elements are built using intricate 3D assets based on real-world references, ensuring accurate representation of structural and material characteristics.

We also simulate different lighting conditions by controlling the depth of the underwater environment. In our experiments, we configure two representative depths to emulate shallow (50m) and deep water (500m)² scenarios. For each task, the starting position is randomly selected to vary task difficulty, because tasks become increasingly challenging when the start point is far from the target, the target is initially out of view, or the initial orientation faces away from the goal. Furthermore, OCEANGYM is completely scalable, allowing users to customize the environment by selecting new depths to simulate more complex lighting conditions, or by adding new props and designing additional tasks based on the existing environment, thereby extending the diversity and difficulty.

2.2 UNDERWATER EMBODIED AGENTS

We model the agent’s control–perception loop as a Partially Observable Markov Decision Process (POMDP) enhanced with contextual memory. At each time step t , the agent processes the task specification $\mathcal{T} = (I_{\text{target}}, c)$, where I_{target} is a visual reference image of the target and c provides its textual identity and features. It also considers language instruction L , synchronized observations O_t , and its memory state m_t . These elements collectively shape the agent’s perception and objectives.

With the above information, the agent must generate either a textual perception response y_t for perception tasks, or determine a control action a_t for decision tasks. Here, $a_t \in \mathcal{A}$ is a discrete action selected from the action space \mathcal{A} . A decision trajectory is described by $\sigma = (O_1, a_1, s_1, m_1, \dots, m_{t-1}, O_t, a_t, s_t)$. In this sequence, O_i represents the observations, a_i the actions, s_i the states, and m_i the memory states at each time step i . The episode concludes when the target is achieved or when the maximum time t_{\max} is exhausted. The ultimate reward is based on the successful score of the task, as defined in §2.5.

²For deep water scenarios, optical sensing relies on artificial light sources, with a visibility range of approximately 0–10m.

State and Observation. The agent's state at time t is given by $s_t = \{(x_t, y_t, z_t), (\phi_t, \theta_t, \psi_t)\}$, where (x_t, y_t, z_t) represent the agent's 3D positional coordinates, and $(\phi_t, \theta_t, \psi_t)$ denote the roll, pitch, and yaw angles, respectively. At each timestep, the agent receives synchronized RGB and sonar images from sensors oriented in six different directions. The directions are defined by the set $\mathcal{D}_{\text{sensor}} = \{\text{f, b, l, r, u, d}\}$, corresponding to front, back, left, right, up, and down. The RGB images from these directions are denoted as $O_t^R = \{o_{t,d}^R\}_{d \in \mathcal{D}_{\text{sensor}}}$, and the sonar images are represented similarly as $O_t^S = \{o_{t,d}^S\}_{d \in \mathcal{D}_{\text{sensor}}}$. Therefore, the complete observation at time t can be expressed as a combination of both image sets, $O_t = (O_t^R, O_t^S)$.

Action Space. The agent's action direction set is defined as $\mathcal{D}_{\text{action}} = \{f, b, l, r, u, d, rl, rr\}$, which encompasses both directional and rotational movements. Directional actions include translations along the primary axes: forward (f), backward (b), left (l), right (r), up (u), and down (d). Rotational actions consist of rotate left (rl) and rotate right (rr). At each timestep t , the agent selects an action $a_t \in \mathcal{A}$ from this discrete set and applies a control magnitude $\delta \in \mathbb{R}_{\geq 0}$ to determine the execution intensity.

Memory. Memory systems play a crucial role in storing and structuring past information, thereby enhancing the agent's resilience in dynamic and partially observable environments (Xi et al., 2025; Liu et al., 2023; Zhong et al., 2024; Wu et al., 2024; Maharana et al., 2024). OCEANGYM agent maintains an explicit memory m_t , structured as a sliding window that records the last K steps:

$$m_t = \{(d_{t-k}, a_{t-k}) \mid k = 1, 2, \dots, K\}. \quad (1)$$

Within this memory structure, d_{t-k} denotes the textual description at time $t-k$, and a_{t-k} represents the corresponding action executed. The sliding window size K is implemented primarily to prevent the context length from exceeding the model's maximum input capacity. The default window size is large enough to capture the necessary historical information for most tasks in our benchmark. The perception module \mathcal{P}_θ , modeled as an MLLM, generates a summary based on the current context and the interaction history $\{(O_k, a_k)\}_{k=t-K}^t$:

$$d_t = \mathcal{P}_\theta(\{(O_k, a_k)\}_{k=t-K}^t). \quad (2)$$

This summary is subsequently used to refresh the memory: $m_{t+1} = \text{update}(m_t, d_t, a_t)$.

Memory-augmented Markov Process. To maintain the Markov property while incorporating memory, we introduce an augmented hidden state $\tilde{s}_t = (s_t, m_t)$. The state transition is then modeled as:

$$p(\tilde{s}_{t+1} \mid \tilde{s}_t, a_t, \delta), \quad (3)$$

where $p(\cdot \mid \cdot)$ represents the augmented state transition function of the environment. This function captures both the evolution of memory, ensuring that the system remains Markovian despite the added complexity of memory integration.

Agent Policy. The agent policy is a multimodal, memory-augmented mapping parameterized by an MLLM with parameter vector θ :

$$\pi_\theta(a_t, y_t \mid L, O_t, m_t, \mathcal{T}, \delta), \quad (4)$$

Concretely, for perception tasks, we sample an answer $y_t \sim \pi_\theta(y \mid L, O_t, m_t, \mathcal{T}, \delta)$, and for decision tasks, we sample an action $a_t \sim \pi_\theta(a \mid L, O_t, m_t, \mathcal{T}, \delta)$. An episode terminates at time T when the agent either outputs a STOP command (for decision tasks) or provides a final answer to the question (for perception tasks) or when the maximum time t_{\max} is reached. The policy, combined with the memory-augmented transition dynamics, induces the trajectory distribution:

$$\mathbb{P}_\theta(\sigma \mid L, \mathcal{T}) = \prod_{t=1}^{T-1} \pi_\theta(a_t, y_t \mid L, O_t, m_t, \mathcal{T}, \delta) p(\tilde{s}_{t+1} \mid \tilde{s}_t, a_t, \delta), \quad (5)$$

where σ represents the trajectory of the agent through the state space over time, influenced by the specified policy π_θ and the transition model $p(\tilde{s}_{t+1} \mid \tilde{s}_t, a_t, \delta)$.

216 2.3 OCEANGYM PERCEPTION TASKS
217218 The perception tasks are categorized into two settings: **Multi-View Perception** and **Context-based**
219 **Perception**. These tasks primarily use RGB images as input, with sonar data added in certain
220 experiments to enhance perception. The data for each setting are collected by human operators and
221 designed to evaluate different aspects of MLLMs' perceptual abilities. There are a total of 85 scenes.
222 More details in Appendix A.3.223 **Multi-view Perception Setting.** This setting evaluates the agent's ability to interpret visual information
224 from multiple synchronized viewpoints. At each timestep t , the agent captures a set of six
225 simultaneous RGB images, denoted as $O_t^R = \{o_{t,d}^R\}_{d \in \mathcal{D}_{\text{sensor}}}$, where d refers to the different sensor
226 orientations: front, back, left, right, up, and down. The objective is to consistently identify
227 and localize underwater objects across these varied viewpoints. This setting examines whether
228 objects visible from certain angles can be correctly perceived when the visual inputs from all directions
229 are sequentially processed by the MLLM, thereby evaluating robustness to viewpoint variations.230 **Context-based Perception Setting.** This setting assesses the agent's ability to perceive and interpret
231 sequential observations gathered during navigation. At each timestep t , the agent captures an RGB
232 image o_t^R from a fixed orientation, forming a chronological sequence $O_{1:m}^R = \{o_t^R\}_{t=1}^m$, where m
233 is the total number of timesteps. The agent must track and understand changes over time, ensuring
234 consistent and accurate identification and localization of underwater objects. This evaluation em-
235 phasizes temporal consistency and the agent's capacity to build a coherent perception from a stable
236 visual perspective in dynamic and complex underwater environments.237 **Running Example: Shipwreck Area**
238239 **Perception Task:** (1) Multi-view perception setting. The agent receives perception images (vi-
240 sual and sonar) from different sensors at the same time to determine the target, such as whether
241 it is a shipwreck. (2) Context-based perception setting. The agent analyzes images one by one
242 along a trajectory from a fixed viewpoint to identify the target.243 **Decision Task:** The agent receives a task instruction, such as "Search for a sunken ship," and
244 then explores the area for 30 minutes to complete it.
245246 2.4 OCEANGYM DECISION TASKS
247248 **Decision Task Definition.** Decision tasks evaluate decision-making in continuous 3D environments,
249 where agents must integrate multimodal sensory input with task specifications. Each episode begins
250 from an initial state $s_0 = \{(x_0, y_0, z_0), (\phi_0, \theta_0, \psi_0)\}$ and requires the agent to reach the target
251 defined by \mathcal{T} . The agent must combine sensory observations O_t , temporal memory, and goal
252 information to execute precise maneuvers in cluttered, low-visibility environments. Key parameters
253 of the task include the decision interval t_{interval} and the task's limited duration t_{max} ³. The decision
254 interval t_{interval} determines how frequently the agent makes decisions and executes actions. The total
255 task duration t_{max} sets the temporal constraint, within which the agent must meet its objectives,
256 thereby influencing the planning and movement strategies employed by the agent. Compared with
257 grid-based navigation benchmarks, this task emphasizes continuous control and realistic underwater
258 environment, reflecting the challenges of autonomous exploration and inspection tasks.259 **Decision Task Design.** To evaluate the decision-making capabilities of MLLMs in marine environments,
260 we design eight representative task scenarios that are commonly used in actual underwater
261 operations (more details in Appendix A.4). The task construction methods are divided into two cat-
262 egories: detection tasks and tracking tasks. Detection tasks focus on assessing the ability of MLLMs
263 to locate specific underwater objects, including searching for large targets such as sunken ships
264 or aircraft wreckage, and smaller targets like scientific research robots. Tracking tasks focus on
265 evaluating the ability of MLLMs to perform inspection and monitoring tasks underwater, including
266 scenarios like pipeline inspection and platform approaches. To further investigate the performance
267 in challenging environments, four representative tasks are conducted under low light deep-sea con-
268 ditions. In the experimental design, a systematic initial positioning strategy is adopted for each
269³By default, t_{interval} takes 30 seconds and t_{max} takes 0.5 hours in decision tasks.

270 Table 1: Performance of perception tasks across different models and conditions. Values represent
 271 accuracy percentages (%). Adding sonar means using both RGB and sonar images.
 272

Model	Shallow Water Environment (High Illumination)						Deep Water Environment (Low Illumination)					
	Multi-View Perception		Context-based Perception		Avg	Multi-View Perception		Context-based Perception		Avg		
	Vision	+Sonar	Vision	+Sonar		Vision	+Sonar	Vision	+Sonar		Vision	+Sonar
GLM-4.5V	52.73	56.36	46.67	63.33	54.77	36.36	30.91	20.00	33.33	30.15		
GPT-4o-mini	34.55	34.55	20.00	33.33	30.61	14.55	20.00	3.33	6.67	11.14		
Gemini-2.5-Flash	29.09	30.91	50.00	33.33	35.83	9.09	5.45	20.00	30.00	16.14		
Qwen2.5-VL-7B	58.18	43.64	56.67	70.00	57.12	27.27	20.00	33.33	33.33	28.48		
Minicpm-4.5	52.73	43.64	36.67	23.33	39.09	29.09	23.64	43.33	13.33	27.35		
Human	100.00	100.00	100.00	100.00	100.00	94.55	98.18	86.67	90.00	92.35		

284 task. The first two starting positions remain consistent across all tasks to ensure experimental re-
 285 producibility. The third starting position is randomly generated within the operational boundary to
 286 evaluate the adaptability of the agent to different initial conditions.

288 2.5 EVALUATION METRICS

289 **Perception Task Evaluation.** We evaluate model performance using exact match accuracy. Let y_i
 290 denote the ground-truth answer and \hat{y}_i represent the model’s predicted answer for the i -th sample.

$$292 \text{Acc} = \frac{100\%}{N} \sum_{i=1}^N \mathbb{I}[\hat{y}_i = y_i], \quad (6)$$

295 For multiple-choice items, y_i and \hat{y}_i are treated as sets and equality requires an exact set match.

296 **Decision Task Evaluation.** We evaluate decision tasks using a distance-based scoring method. Each
 297 episode ends when the agent issues a STOP command or reaches the time limit t_{\max} . For a task with n
 298 evaluation points, let \mathbf{p}_i be the i -th target location. If the target is detected, we use the closest position
 299 from the agent’s trajectory to \mathbf{p}_i ; otherwise, we use the agent’s final position. The Euclidean distance
 300 is computed as $d_i = \|\hat{\mathbf{p}}_i - \mathbf{p}_i\|_2$, and the score for each point is defined as:

$$302 S_i = \begin{cases} 100, & d_i \leq \tau_1, \\ 100 \frac{\tau_2 - d_i}{\tau_2 - \tau_1}, & \tau_1 < d_i \leq \tau_2, \\ 0, & d_i > \tau_2, \end{cases} \quad (7)$$

307 where the distance thresholds are set to $\tau_1 = 30$ meters and $\tau_2 = 100$ meters by default. The total
 308 score is a weighted sum as $S_{\text{total}} = \sum_{i=1}^n w_i S_i$, where w_i are task-specific weights⁴.

310 3 EXPERIMENTS

312 3.1 EXPERIMENTAL SETTINGS

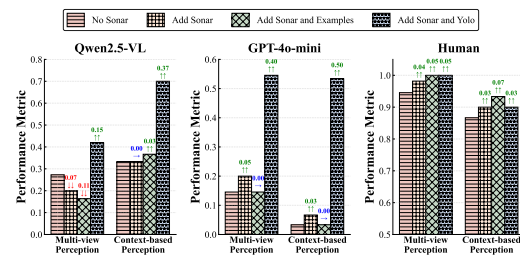
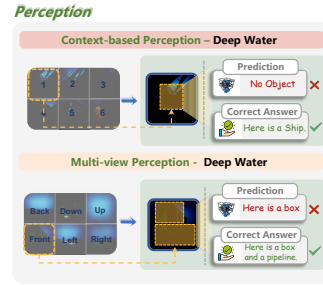
314 To thoroughly evaluate the perception and decision capabilities of MLLMs in underwater environments,
 315 we conduct experiments using a variety of models⁵. Among the open-source models, we
 316 assess MiniCPM-V-4.5 (Yao et al., 2025), GLM-4.5V (Team et al., 2025) and Qwen2.5-VL-7B (Bai
 317 et al., 2025). For proprietary models, we test GPT-4o-mini (OpenAI, 2024) and Gemini-2.5-Flash
 318 (Gemini Team, 2024). **We run each task three times and report the average results.** Humans pro-
 319 vide perception and decision-making answers based on tasks, and operate underwater robots through
 320 keyboards for decision-making tasks.

321 ⁴For a single-point task $w_1 = 1.0$; for two points $(w_1, w_2) = (0.6, 0.4)$; for three points $(w_1, w_2, w_3) =$
 322 $(0.6, 0.2, 0.2)$.

323 ⁵Note that our setup is designed to real-world deployment of MLLMs in the future; accordingly, we priori-
 324 tize smaller-scale models that can run natively on edge devices.

324 Table 2: Performance in decision tasks requiring autonomous completion by MLLM-driven agents.
325

326 327 328 329 330 331 332 333 334 335 336 337 338 339 340 341 342 343 344 345 346 347 348 349 350 351 352 353 354 355 356 357 358 359 360 361 362 363 364 365 366 367 368 369 370 371 372 373 374 375 376 377	326 327 328 329 330 331 332 333 334 335 336 337 338 339 340 341 342 343 344 345 346 347 348 349 350 351 352 353 354 355 356 357 358 359 360 361 362 363 364 365 366 367 368 369 370 371 372 373 374 375 376 377				Model
Task	GLM-4.5V	GPT-4o-mini	Gemini-2.5	Qwen2.5-VL-7B	Human
Shallow Water Environment (High Illumination)					
Locate the robot	6.6 \pm 19.83	8.9 \pm 10.1	0.0 \pm 0.00	7.8 \pm 13.5	100
Locate the oil drums	10.7 \pm 16.52	11.1 \pm 19.2	3.5 \pm 6.0	5.7 \pm 9.8	100
Locate the electrical box	7.9 \pm 17.08	36.6 \pm 21.9	15.9 \pm 27.4	8.7 \pm 15.0	100
Search for a sunken ship	5.9 \pm 5.04	13.4 \pm 19.3	20.5 \pm 14.3	10.3 \pm 10.3	100
Search for the aircraft	25.0 \pm 6.10	16.9 \pm 17.8	11.7 \pm 15.6	7.8 \pm 10.0	100
Inspect oil pipe	37.8 \pm 17.88	27.1 \pm 23.6	18.3 \pm 15.8	30.8 \pm 25.2	100
Inspect the wind turbine	20.3 \pm 28.89	13.9 \pm 14.33	25.1 \pm 22.1	14.7 \pm 17.0	100
Docking	14.9 \pm 13.20	19.2 \pm 33.28	19.4 \pm 33.6	8.3 \pm 7.2	100
Average	16.1 \pm 15.6	18.4 \pm 19.9	14.4 \pm 16.1	11.8 \pm 13.7	100
Deep Water Environment (Low Illumination)					
Locate oil drums		10.6 \pm 21.35	5.6 \pm 9.69	0.0 \pm 0.0	0.0 \pm 0.0
Search for a sunken ship		2.9 \pm 2.16	12.8 \pm 14.48	8.2 \pm 14.1	3.4 \pm 5.8
Inspect the oil pipe		32.5 \pm 5.86	15.8 \pm 15.5	6.6 \pm 11.4	21.7 \pm 25.3
Inspect the wind turbine		0.0 \pm 0.0	25.1 \pm 16.0	10.6 \pm 10.0	0.4 \pm 0.6
Average		11.5 \pm 7.3	14.8 \pm 13.9	6.4 \pm 8.8	6.4 \pm 8.4

353 Figure 3: Performance comparison between human
354 and MLLMs after adding sonar and sonar reference
355 examples for objects in deep water environments.353 Figure 4: Case analysis in perception tasks.
354 Agents are susceptible to perception errors under
355 challenging conditions such as low-light environments,
356 multi-object scenarios, and occlusions.357

3.2 MAIN RESULTS

358 **Perception Results.** The results for perception tasks are summarized in Table 1. In shallow, well-
359 illuminated water environments, Qwen2.5-VL-7B achieves the strongest overall performance among
360 the evaluated MLLMs, with an average accuracy of 57.12%, while GLM-4.5V demonstrates com-
361 petitive performance with 54.77% average accuracy. Multi-view perception generally yields higher
362 accuracy than the context-based setting across most models, likely because targets of similar size
363 across viewpoints are easier to interpret, whereas distant objects in sequential views can introduce
364 ambiguity. Under deep water conditions with low illumination, all models exhibit significant per-
365 formance degradation, though GLM-4.5V emerges as the most robust (30.15% average accuracy),
366 followed by Qwen2.5-VL-7B (28.48%) and Minicpm-4.5 (27.35%). Notably, incorporating sonar
367 data does not consistently improve performance across models or tasks (further analysis in §3.3).

368 **Decision Results.** Performance on decision tasks is shown in Table 2. Several tasks resulted in
369 zero scores, indicating extreme difficulty due to small object size or time constraints. GPT-4o-mini
370 achieves the best average performance in both shallow (18.4%) and deep water (14.8%) environ-
371 ments, with GLM-4.5V ranking second under shallow conditions (16.1%) and deep water conditions
372 (11.5%). Performance declines markedly in deep water, where Gemini-2.5 and Qwen2.5-VL-7B
373 both average 6.4%. Notably, GLM-4.5V demonstrates strong performance in specific tasks, achiev-
374 ing the highest scores in "Search for the aircraft" (25.0%) and "Inspect oil pipe" (37.8%) in shallow
375 water, and "Inspect the oil pipe" (32.5%) in deep water. Human performance substantially outper-
376 forms all models, reaching 100% in shallow water and 69.6% in deep water, underscoring the gap
377 between current MLLM-driven decision-making and human proficiency.

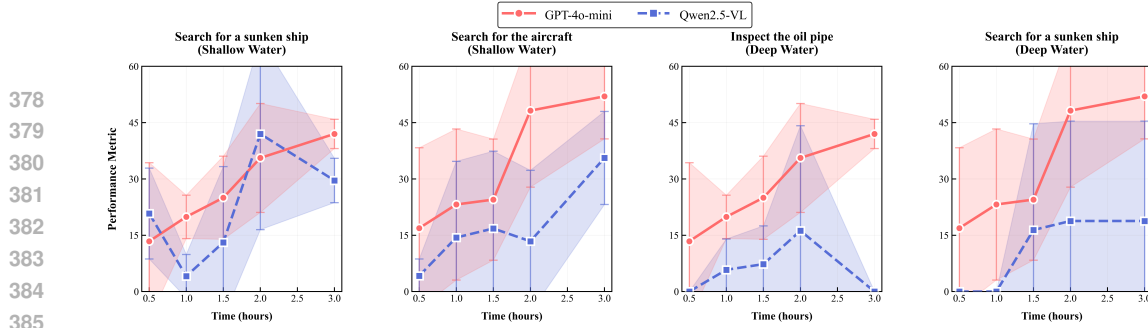


Figure 5: Scaling analysis performance over time in decision tasks.

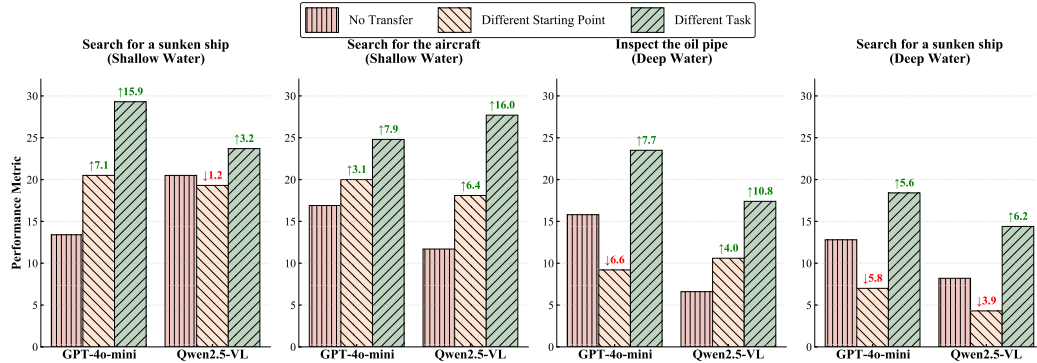


Figure 6: Impact of different memory transfer mechanisms on model performance.

3.3 ANALYSIS

MLLM agents struggle to exploit sonar data for enhanced underwater perception, in stark contrast to humans who leverage it effectively. To investigate the role of sonar data in deep-water environments, we compare the performance of human experts with the two MLLMs, Qwen2.5-VL and GPT-4o-mini, on perception tasks. Specifically, we either let the models directly comprehend sonar images or provide them with human-annotated interpretations as prompts. As shown in Figure 3, human experts consistently benefit from incorporating sonar data across tasks. By contrast, MLLMs exhibit only limited gains when using raw sonar images, and this gap becomes even more pronounced when reference sonar images of each object are introduced. This limitation likely stems from current MLLMs’ fundamental difficulty in interpreting sonar imagery and underwater perceptual data (Xie et al., 2022; Zheng et al., 2023; Xu et al., 2025; Aubard et al., 2025), combined with potential constraints in the sonar simulation within OceanGym, an issue we discuss in §3.3. Notably, when employing a YOLO model (Redmon et al., 2016) specifically trained on sonar data as auxiliary perception tools, we observe significant performance improvements, suggesting that specialized vision models may currently outperform general-purpose MLLMs in sonar data interpretation tasks.

Extended exploration enhances an agent’s acquisition of environmental knowledge and task performance, following a scaling law that eventually plateaus. We analyze the relationship between navigation performance and operational duration using the representative MLLMs, across both shallow- and deep-water scenarios. The performance was evaluated over durations of 0.5, 1, 1.5, 2, and 3 hours. As shown in Figure 5, performance initially improves with longer operation time, consistent with prior studies on test-time scaling (Zhang et al., 2025a; Zhu et al., 2025), but eventually plateaus. This plateau reflects inherent limitations in perception, memory, and reasoning, as well as a lack of intrinsic curiosity to explore new regions. These findings underscore the need to improve both fundamental MLLM capabilities and agent strategies, such as enhanced memory and long-horizon planning, to break through performance ceilings in embodied environments.

Memory transfer enables agents to leverage past experience to tackle new challenges. We investigate whether knowledge and experience accumulated from previous tasks (Hou et al., 2024; Hu et al., 2024a; Tan et al., 2025; Tang et al., 2025) can enhance performance in new tasks. Specifically, we explore using agents’ previously explored trajectories as experiential input. Experiments are conducted in both shallow water and deep water environments, evaluating two transfer conditions: within-task transfer (different starting points) and cross-task transfer (different but related tasks). As

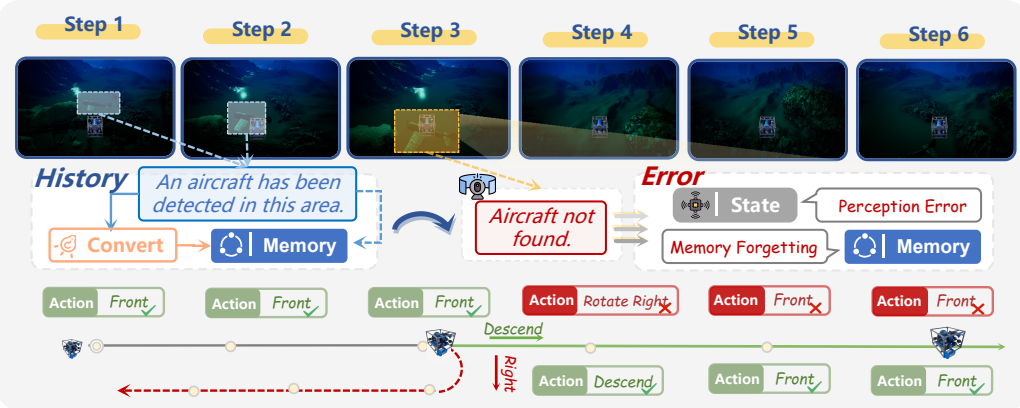
Navigation

Figure 7: Case analysis in decision tasks.

shown in Figure 6, memory transfer improves decision-making performance in shallow water environments under both transfer conditions. However, in the more challenging deep water environment, only cross-task transfer demonstrates stable performance improvements, while within-task transfer shows limited benefits. This suggests that more appropriate prior experiences provide more robust guidance under perceptually degraded conditions. Transfer learning helps compensate for perceptual limitations by providing informed priors about environmental structure and effective navigation strategies. These findings underscore the importance of developing adaptive memory retrieval mechanisms that can selectively leverage relevant past experiences to enhance decision-making in autonomous underwater agents operating under diverse environmental conditions.

Case analysis. We present case analyses and illustrate failure cases in Figure 4, mainly due to: (1) **Occlusions**, where targets are partially blocked; (2) **Multi-object Scenes**, causing identification and localization ambiguities; and (3) **Low Illumination**, which severely reduces vision-based perception accuracy. Figure 7 shows common decision task failures, primarily from: (1) **Perception Errors**, where inaccurate detection leads to wrong actions; and (2) **Memory Forgetting**, where the agent cannot retain crucial past information, such as visited locations or previous decisions. Furthermore, we deploy physical objects that serve as real-world references for object modeling in OceanGym into an actual marine environment to correlate simulated performance with real-world performance. An AUV equipped with a sonar data acquisition system is then used to collect sonar measurements. As shown in the Figure 8, **the YOLO model trained in the simulated environment enhances GPT-4o-mini’s ability to interpret real-world sonar data**. However, it exhibits limited generalization capability for objects not included in the simulation.

Discusses and Limitations of OCEANGYM. OCEANGYM offers a versatile testbed for underwater embodied agents, though it cannot fully replicate real-world conditions as factors like currents, salinity, marine life, and sonar noise remain imperfectly modeled. Despite these constraints, OCEANGYM supports synthetic data generation and facilitates reinforcement learning with rich feedback, and serves as a sim-to-real bridge for deploying models on AUVs (See §A.2).

4 RELATED WORK

Embodied Simulations. Embodied intelligence describes artificial intelligence systems whose intelligent behavior emerges through continuous physical and sensory interactions with the environment (Gupta et al., 2021; Ding et al., 2024; Shi et al., 2024). Simulation platforms are essential for advancing such systems across ground, aerial, and marine domains (Liu et al., 2024b; Han et al., 2025; Aldhaheri et al., 2025). In ground applications, platforms like Matterport3D (Chang et al., 2017), House3D (Wu et al., 2018), and Habitat (Manolis Savva et al., 2019) provide realistic indoor and outdoor environments for navigation, scene understanding, and human-robot interaction research. Aerial robotics benefits from simulators such as AirSim (Shah et al., 2018), CityNav (Lee et al., 2025) and OpenUAV (Wang et al., 2024a), which offer high-fidelity simulations with accurate physics and sensor models. Similarly, in the marine domain, simulation platforms such as HoloOcean (Potokar et al., 2022), OceanSim (Song et al., 2025), and MarineGym (Chu et al., 2025) provide specialized capabilities for modeling hydrodynamic effects and underwater dynamics. With the development of embodied intelligence, an increasing variety of simulation environments (Kolve

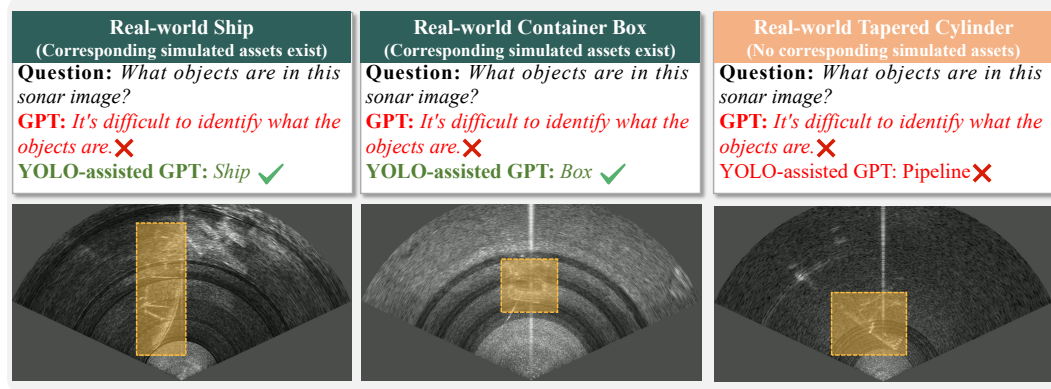


Figure 8: We evaluate whether YOLO models trained in simulated environments can enhance real-world performance by testing them on actual sonar data. The results demonstrate that while the YOLO-assisted GPT-4o-mini approach yields measurable performance improvements for certain objects modeled in OceanGym, the models exhibit limited generalization capability for objects not included in the simulation.

et al., 2017; Puig et al., 2018; Xiang et al., 2020; Gan et al., 2021; Li et al., 2021; Nasiriany et al., 2024; Zhou et al., 2024b; Hong et al., 2025) have emerged to meet specific tasks, needs, or scenarios.

MLLM-driven Embodied Agents. Building upon the rapid advancement of LLMs (Achiam et al., 2023; Touvron et al., 2023; Chiang et al., 2023; Yang et al., 2025a), the emergence of MLLMs (OpenAI, 2024; Bai et al., 2025; Meta AI, 2024; Liu et al., 2024a; Gemini Team, 2024; Team et al., 2025; Wang et al., 2025b) has further strengthened agent capabilities by incorporating visual understanding for multimodal perception. Despite impressive results in various agent applications (Hu et al., 2024b; Ning et al., 2025), MLLM-driven agents still face substantial challenges in real-world and simulated embodied environments. Key difficulties persist in spatial cognition (Prasad et al., 2023; Du et al., 2024; Tong et al., 2024; Shiri et al., 2024; Zheng et al., 2024; Dang et al., 2025; Yang et al., 2025c; Li et al., 2025), task planning (Chen et al., 2023; Huang et al., 2023; Zhou et al., 2024a), object navigation (Wang et al., 2024b; Khanna et al., 2024; Guo et al., 2025; Qiao et al., 2025; Cheng et al., 2025), and robotic manipulation (Zheng et al., 2022a; Yang et al., 2025b; Wang et al., 2025a). To evaluate agent capabilities, embodied benchmarks have been developed across diverse settings, including indoor (Anderson et al., 2018; Wu et al., 2018), urban (Chen et al., 2019; Caesar et al., 2020; Vasudevan et al., 2021; Gao et al., 2024), aerial (Yao et al., 2024; Gao et al., 2025b; Cai et al., 2025), specialised (Zheng et al., 2022b; Luo et al., 2023; Song et al., 2024; Li et al., 2024a) and real-world (Zhao et al., 2025; Koh et al., 2024; Zhang et al., 2025b) scenarios.

5 CONCLUSION

We introduce OCEANGYM, the first benchmark environment specifically designed for underwater embodied agents. Our experiments reveal significant limitations in current MLLMs. We hope OCEANGYM can bridge the gap between simulated research and real-world deployment, offering a foundation for developing robust autonomous systems for marine applications.

ETHICS STATEMENT

This research is conducted in strict compliance with established ethical guidelines and best practices in scientific research. All data employed in this study are obtained from publicly accessible datasets, with no utilization of proprietary or confidential information. Proper and accurate citations are provided for all data sources referenced throughout this paper. We emphatically advise all users to maintain the highest ethical standards when utilizing our dataset, ensuring principles of fairness, transparency, and responsibility in their research applications. Any use of the dataset that may potentially cause harm or adversely affect societal welfare is expressly prohibited.

REPRODUCIBILITY STATEMENT

We provide data from our benchmark under file size limitation, along with the corresponding evaluation code, in the supplementary materials. Detailed descriptions of the environment setup and data construction procedures are available in § 2.1, § 2.3 and § 2.4. Additional data details and

540 comprehensive benchmark statistics can be found in Appendix A.3 and Appendix A.4. Specific
 541 configurations of the tested models are documented in Section 3.1.
 542

543 **REFERENCES**
 544

545 Josh Achiam, Steven Adler, Sandhini Agarwal, Lama Ahmad, Ilge Akkaya, Florencia Leoni Ale-
 546 man, Diogo Almeida, Janko Altenschmidt, Sam Altman, Shyamal Anadkat, et al. Gpt-4 technical
 547 report. *arXiv preprint arXiv:2303.08774*, 2023.

548 Sara Aldhaheri, Yang Hu, Yongchang Xie, Peng Wu, Dimitrios Kanoulas, and Yuanchang Liu. Un-
 549 derwater robotic simulators review for autonomous system development, 2025. URL <https://arxiv.org/abs/2504.06245>.

550

551 Peter Anderson, Qi Wu, Damien Teney, Jake Bruce, Mark Johnson, Niko Sünderhauf, Ian Reid,
 552 Stephen Gould, and Anton van den Hengel. Vision-and-language navigation: Interpreting
 553 visually-grounded navigation instructions in real environments. In *Proceedings of the IEEE Con-
 554 ference on Computer Vision and Pattern Recognition (CVPR)*, 2018.

555

556 Martin Aubard, Ana Madureira, Luís Teixeira, and José Pinto. Sonar-based deep learning in un-
 557 derwater robotics: Overview, robustness, and challenges. *IEEE Journal of Oceanic Engineering*,
 558 2025.

559

560 Shuai Bai, Keqin Chen, Xuejing Liu, Jialin Wang, Wenbin Ge, Sibo Song, Kai Dang, Peng Wang,
 561 Shijie Wang, Jun Tang, Humen Zhong, Yuanzhi Zhu, Ming-Hsuan Yang, Zhaohai Li, Jianqiang
 562 Wan, Pengfei Wang, Wei Ding, Zheren Fu, Yiheng Xu, Jiabo Ye, Xi Zhang, Tianbao Xie, Zesen
 563 Cheng, Hang Zhang, Zhibo Yang, Haiyang Xu, and Junyang Lin. Qwen2.5-vl technical report.
 564 *CoRR*, abs/2502.13923, 2025. doi: 10.48550/ARXIV.2502.13923. URL <https://doi.org/10.48550/arXiv.2502.13923>.

565

566 Philip J Ball, J Bauer, F Belletti, et al. Genie 3: A new frontier for world models, 2025.

567

568 Holger Caesar, Varun Bankiti, Alex H Lang, Sourabh Vora, Venice Erin Liong, Qiang Xu, Anush
 569 Krishnan, Yu Pan, Giancarlo Baldan, and Oscar Beijbom. nuscenes: A multimodal dataset for
 570 autonomous driving. In *Proceedings of the IEEE/CVF conference on computer vision and pattern
 recognition*, pp. 11621–11631, 2020.

571

572 Hengxing Cai, Jinhan Dong, Jingjun Tan, Jingcheng Deng, Sihang Li, Zhifeng Gao, Haidong
 573 Wang, Zicheng Su, Agachai Sumalee, and Renxin Zhong. Flightgpt: Towards generalizable
 574 and interpretable UAV vision-and-language navigation with vision-language models. *CoRR*,
 575 abs/2505.12835, 2025. doi: 10.48550/ARXIV.2505.12835. URL <https://doi.org/10.48550/arXiv.2505.12835>.

576

577 Angel Chang, Angela Dai, Thomas Funkhouser, Maciej Halber, Matthias Niessner, Manolis Savva,
 578 Shuran Song, Andy Zeng, and Yinda Zhang. Matterport3D: Learning from RGB-D data in indoor
 579 environments. *International Conference on 3D Vision (3DV)*, 2017.

580

581 Howard Chen, Alane Suhr, Dipendra Misra, Noah Snavely, and Yoav Artzi. Touchdown: Natural
 582 language navigation and spatial reasoning in visual street environments. In *2019 IEEE/CVF
 583 Conference on Computer Vision and Pattern Recognition (CVPR)*, pp. 12530–12539, 2019. doi:
 10.1109/CVPR.2019.01282.

584

585 Yaran Chen, Wenbo Cui, Yuanwen Chen, Mining Tan, Xinyao Zhang, Dongbin Zhao, and He Wang.
 586 Robogpt: an intelligent agent of making embodied long-term decisions for daily instruction tasks.
 587 *arXiv preprint arXiv:2311.15649*, 2023.

588

589 Zhili Cheng, Yuge Tu, Ran Li, Shiqi Dai, Jinyi Hu, Shengding Hu, Jiahao Li, Yang Shi, Tianyu Yu,
 590 Weize Chen, et al. Embodiedeval: Evaluate multimodal llms as embodied agents. *arXiv preprint
 arXiv:2501.11858*, 2025.

591

592 Wei-Lin Chiang, Zhuohan Li, Zi Lin, Ying Sheng, Zhanghao Wu, Hao Zhang, Lianmin Zheng,
 593 Siyuan Zhuang, Yonghao Zhuang, Joseph E. Gonzalez, Ion Stoica, and Eric P. Xing. Vicuna: An
 open-source chatbot impressing gpt-4 with 90%* chatgpt quality, March 2023. URL <https://lmsys.org/blog/2023-03-30-vicuna/>.

594 Shuguang Chu, Zebin Huang, Yutong Li, Mingwei Lin, Ignacio Carlucho, Yvan R. Petillot, and
 595 Canjun Yang. Marinegym: A high-performance reinforcement learning platform for underwater
 596 robotics, 2025. URL <https://arxiv.org/abs/2503.09203>.

597 Ronghao Dang, Yuqian Yuan, Yunxuan Mao, Kehan Li, Jiangpin Liu, Zhikai Wang, Xin Li, Fan
 598 Wang, and Deli Zhao. Rynnec: Bringing mllms into embodied world, 2025. URL <https://arxiv.org/abs/2508.14160>.

600 Jingtao Ding, Yunke Zhang, Yu Shang, Yuheng Zhang, Zefang Zong, Jie Feng, Yuan Yuan,
 601 Hongyuan Su, Nian Li, Nicholas Sukiennik, et al. Understanding world or predicting future?
 602 a comprehensive survey of world models. *arXiv preprint arXiv:2411.14499*, 2024.

603 Mengfei Du, Binhao Wu, Zejun Li, Xuanjing Huang, and Zhongyu Wei. Embsspatial-bench: Bench-
 604 marking spatial understanding for embodied tasks with large vision-language models. *CoRR*,
 605 abs/2406.05756, 2024. doi: 10.48550/ARXIV.2406.05756. URL <https://doi.org/10.48550/arXiv.2406.05756>.

606 Epic Games. Unreal engine, 2025. URL <https://www.unrealengine.com>.

607 Pascale Fung, Yoram Bachrach, Asli Celikyilmaz, Kamalika Chaudhuri, Delong Chen, Willy Chung,
 608 Emmanuel Dupoux, Hongyu Gong, Hervé Jégou, Alessandro Lazaric, et al. Embodied ai agents:
 609 Modeling the world. *arXiv preprint arXiv:2506.22355*, 2025.

610 Chuang Gan, Jeremy Schwartz, Seth Alter, Damian Mrowca, Martin Schrimpf, James Traer,
 611 Julian De Freitas, Jonas Kubilius, Abhishek Bhandwaldar, Nick Haber, Megumi Sano,
 612 Kuno Kim, Elias Wang, Michael Lingelbach, Aidan Curtis, Kevin T. Feiglis, Daniel
 613 Bear, Dan Gutfreund, David D. Cox, Antonio Torralba, James J. DiCarlo, Josh Tenen-
 614 baum, Josh H. McDermott, and Dan Yamins. Threedworld: A platform for interactive
 615 multi-modal physical simulation. In Joaquin Vanschoren and Sai-Kit Yeung (eds.), *Pro-
 616 ceedings of the Neural Information Processing Systems Track on Datasets and Bench-
 617 marks 1, NeurIPS Datasets and Benchmarks 2021, December 2021, virtual*, 2021. URL
 618 <https://datasets-benchmarks-proceedings.neurips.cc/paper/2021/hash/735b90b4568125ed6c3f678819b6e058-Abstract-round1.html>.

619 Chen Gao, Baining Zhao, Weichen Zhang, Jinzhu Mao, Jun Zhang, Zhiheng Zheng, Fanhang Man,
 620 Jianjie Fang, Zile Zhou, Jinqiang Cui, Xinlei Chen, and Yong Li. Embodiedcity: A benchmark
 621 platform for embodied agent in real-world city environment, 2024. URL <https://arxiv.org/abs/2410.09604>.

622 Yuan Gao, Ruiqi Shu, Hao Wu, Fan Xu, Yanfei Xiang, Ruijian Gou, Qingsong Wen, Xian Wu, and
 623 Xiaomeng Huang. Neuralom: Neural ocean model for subseasonal-to-seasonal simulation. *arXiv
 624 preprint arXiv:2505.21020*, 2025a.

625 Yunpeng Gao, Chenhui Li, Zhongrui You, Junli Liu, Zhen Li, Pengan Chen, Qizhi Chen, Zhonghan
 626 Tang, Liansheng Wang, Penghui Yang, Yiwen Tang, Yuhang Tang, Shuai Liang, Songyi Zhu,
 627 Ziqin Xiong, Yifei Su, Xinyi Ye, Jianan Li, Yan Ding, Dong Wang, Zhigang Wang, Bin Zhao, and
 628 Xuelong Li. Openfly: A comprehensive platform for aerial vision-language navigation, 2025b.
 629 URL <https://arxiv.org/abs/2502.18041>.

630 Gemini Team. Gemini: A family of highly capable multimodal models, 2024.

631 Mingning Guo, Mengwei Wu, Jiarun He, Shaoxian Li, Haifeng Li, and Chao Tao. BEDI: A com-
 632 prehensive benchmark for evaluating embodied agents on uavs. *CoRR*, abs/2505.18229, 2025.
 633 doi: 10.48550/ARXIV.2505.18229. URL <https://doi.org/10.48550/arXiv.2505.18229>.

634 Agrim Gupta, Silvio Savarese, Surya Ganguli, and Li Fei-Fei. Embodied intelligence via learning
 635 and evolution. *Nature communications*, 12(1):5721, 2021.

636 Xiaofeng Han, Shunpeng Chen, Zenghuang Fu, Zhe Feng, Lue Fan, Dong An, Changwei Wang,
 637 Li Guo, Weiliang Meng, Xiaopeng Zhang, Rongtao Xu, and Shibiao Xu. Multimodal fusion and
 638 vision-language models: A survey for robot vision. *CoRR*, abs/2504.02477, 2025. doi: 10.48550/
 639 ARXIV.2504.02477. URL <https://doi.org/10.48550/arXiv.2504.02477>.

648 Yining Hong, Rui Sun, Bingxuan Li, Xingcheng Yao, Maxine Wu, Alexander Chien, Da Yin,
 649 Ying Nian Wu, Zhecan James Wang, and Kai-Wei Chang. Embodied web agents: Bridging
 650 physical-digital realms for integrated agent intelligence. *CoRR*, abs/2506.15677, 2025. doi: 10.
 651 48550/ARXIV.2506.15677. URL <https://doi.org/10.48550/arXiv.2506.15677>.

652 Yuki Hou, Haruki Tamoto, and Homei Miyashita. "my agent understands me better": Integrating
 653 dynamic human-like memory recall and consolidation in llm-based agents. In *Extended Abstracts*
 654 of the CHI Conference on Human Factors in Computing Systems

655, pp. 1–7, 2024.

656 Mengkang Hu, Tianxing Chen, Qiguang Chen, Yao Mu, Wenqi Shao, and Ping Luo. Hiagent: Hier-
 657 archical working memory management for solving long-horizon agent tasks with large language
 658 model, 2024a.

659 Xueyu Hu, Tao Xiong, Biao Yi, Zishu Wei, Ruixuan Xiao, Yurun Chen, Jiasheng Ye, Meiling Tao,
 660 Xiangxin Zhou, Ziyu Zhao, Yuhuai Li, Shengze Xu, Shawn Wang, Xinchen Xu, Shuofei Qiao,
 661 Kun Kuang, Tieyong Zeng, Liang Wang, Jiwei Li, Yuchen Eleanor Jiang, Wangchunshu Zhou,
 662 Guoyin Wang, Keting Yin, Zhou Zhao, Hongxia Yang, Fan Wu, Shengyu Zhang, and Fei Wu. Os
 663 agents: A survey on mllm-based agents for general computing devices use. <https://github.com/OS-Agent-Survey/OS-Agent-Survey/>, 2024b.

664 Jiangyong Huang, Silong Yong, Xiaojian Ma, Xiongkun Linghu, Puhao Li, Yan Wang, Qing Li,
 665 Song-Chun Zhu, Baoxiong Jia, and Siyuan Huang. An embodied generalist agent in 3d world.
 666 *arXiv preprint arXiv:2311.12871*, 2023.

667 Rachel Kelly, Laura G Elsler, Andrei Polejjack, Sander van der Linden, Kajsa Tönnesson, Sarah E
 668 Schoedinger, Francesca Santoro, Gretta T Pecl, Michael Palmgren, Patrizio Mariani, et al. Em-
 669 powering young people with climate and ocean science: Five strategies for adults to consider. *One
 670 Earth*, 5(8):861–874, 2022.

671 Mukul Khanna, Ram Ramrakhya, Gunjan Chhablani, Sriram Yenamandra, Theophile Gervet,
 672 Matthew Chang, Zsolt Kira, Devendra Singh Chaplot, Dhruv Batra, and Roozbeh Mottaghi. Goat-
 673 bench: A benchmark for multi-modal lifelong navigation. In *Proceedings of the IEEE/CVF Con-
 674 ference on Computer Vision and Pattern Recognition*, pp. 16373–16383, 2024.

675 Jing Yu Koh, Robert Lo, Lawrence Jang, Vikram Duvvur, Ming Chong Lim, Po-Yu Huang, Graham
 676 Neubig, Shuyan Zhou, Ruslan Salakhutdinov, and Daniel Fried. Visualwebarena: Evaluating
 677 multimodal agents on realistic visual web tasks. *arXiv preprint arXiv:2401.13649*, 2024.

678 Eric Kolve, Roozbeh Mottaghi, Winson Han, Eli VanderBilt, Luca Weihs, Alvaro Herrasti, Matt
 679 Deitke, Kiana Ehsani, Daniel Gordon, Yuke Zhu, et al. Ai2-thor: An interactive 3d environment
 680 for visual ai. *arXiv preprint arXiv:1712.05474*, 2017.

681 Jungdae Lee, Taiki Miyanishi, Shuhei Kurita, Koya Sakamoto, Daichi Azuma, Yutaka Matsuo, and
 682 Nakamasa Inoue. Citynav: A large-scale dataset for real-world aerial navigation, 2025. URL
 683 <https://arxiv.org/abs/2406.14240>.

684 Chengshu Li, Fei Xia, Roberto Martín-Martín, Michael Lingelbach, Sanjana Srivastava, Bokui Shen,
 685 Kent Vainio, Cem Gokmen, Gokul Dharan, Tanish Jain, et al. igibson 2.0: Object-centric simula-
 686 tion for robot learning of everyday household tasks. *arXiv preprint arXiv:2108.03272*, 2021.

687 Chengshu Li, Ruohan Zhang, Josiah Wong, Cem Gokmen, Sanjana Srivastava, Roberto Martín-
 688 Martín, Chen Wang, Gabrael Levine, Wensi Ai, Benjamin Jose Martinez, Hang Yin, Michael Lin-
 689 gelbach, Minjune Hwang, Ayano Hiranaka, Sujay Garlanka, Arman Aydin, Sharon Lee, Jiankai
 690 Sun, Mona Anvari, Manasi Sharma, Dhruva Bansal, Samuel Hunter, Kyu-Young Kim, Alan Lou,
 691 Caleb R. Matthews, Ivan Villa-Renteria, Jerry Huayang Tang, Claire Tang, Fei Xia, Yunzhu Li,
 692 Silvio Savarese, Hyowon Gweon, C. Karen Liu, Jiajun Wu, and Li Fei-Fei. BEHAVIOR-1K:
 693 A human-centered, embodied AI benchmark with 1, 000 everyday activities and realistic sim-
 694 ulation. *CoRR*, abs/2403.09227, 2024a. doi: 10.48550/ARXIV.2403.09227. URL <https://doi.org/10.48550/arXiv.2403.09227>.

695 Yun Li, Yiming Zhang, Tao Lin, Xiangrui Liu, Wenxiao Cai, Zheng Liu, and Bo Zhao. Sti-bench:
 696 Are mllms ready for precise spatial-temporal world understanding?, 2025. URL <https://arxiv.org/abs/2503.23765>.

702 Zhe Li, Ronghui Xu, Jilin Hu, Zhong Peng, Xi Lu, Chenjuan Guo, and Bin Yang. Ocean significant
 703 wave height estimation with spatio-temporally aware large language models. In *Proceedings of*
 704 *the 33rd ACM International Conference on Information and Knowledge Management*, pp. 3892–
 705 3896, 2024b.

706 Zikang Li, Zhuojun Xie, Puhong Duan, Xudong Kang, and Shutao Li. Dual spatial attention network
 707 for underwater object detection with sonar imagery. *IEEE Sensors Journal*, 24(5):6998–7008,
 708 2024c.

710 Haotian Liu, Chunyuan Li, Yuheng Li, Bo Li, Yuanhan Zhang, Sheng Shen, and Yong Jae Lee.
 711 Llava-next: Improved reasoning, ocr, and world knowledge, January 2024a. URL <https://llava-vl.github.io/blog/2024-01-30-llava-next/>.

713 Huaping Liu, Di Guo, and Angelo Cangelosi. Embodied intelligence: A synergy of morphology,
 714 action, perception and learning. *ACM Computing Surveys*, 57(7):1–36, 2025.

716 Lei Liu, Xiaoyan Yang, Yue Shen, Binbin Hu, Zhiqiang Zhang, Jinjie Gu, and Guannan Zhang.
 717 Think-in-memory: Recalling and post-thinking enable llms with long-term memory, 2023.

718 Yang Liu, Weixing Chen, Yongjie Bai, Xiaodan Liang, Guanbin Li, Wen Gao, and Liang Lin. Align-
 719 ing cyber space with physical world: A comprehensive survey on embodied ai, 2024b. URL
 720 <https://arxiv.org/abs/2407.06886>.

722 Jianlan Luo, Charles Xu, Fangchen Liu, Liam Tan, Zipeng Lin, Jeffrey Wu, Pieter Abbeel, and
 723 Sergey Levine. Fmb: a functional manipulation benchmark for generalizable robotic learning.
 724 *The International Journal of Robotics Research*, pp. 02783649241276017, 2023.

725 Dong Ma, Ye Li, Teng Ma, and António M Pascoal. The state of the art in key technologies for
 726 autonomous underwater vehicles: A review. *Engineering*, 2025a.

728 Yunsheng Ma, Wenqian Ye, Can Cui, Haiming Zhang, Shuo Xing, Fucui Ke, Jinhong Wang,
 729 Chenglin Miao, Jintai Chen, Hamid Rezatofighi, et al. Position: Prospective of autonomous
 730 driving-multimodal llms world models embodied intelligence ai alignment and mamba. In *Pro-
 ceedings of the Winter Conference on Applications of Computer Vision*, pp. 1010–1026, 2025b.

732 Adyasha Maharana, Dong-Ho Lee, Sergey Tulyakov, Mohit Bansal, Francesco Barbieri, and Yuwei
 733 Fang. Evaluating very long-term conversational memory of llm agents, 2024.

734 Manolis Savva, Abhishek Kadian, Oleksandr Maksymets, Yili Zhao, Erik Wijmans, Bhavana Jain,
 735 Julian Straub, Jia Liu, Vladlen Koltun, Jitendra Malik, Devi Parikh, and Dhruv Batra. Habitat: A
 736 Platform for Embodied AI Research. In *Proceedings of the IEEE/CVF International Conference
 737 on Computer Vision (ICCV)*, 2019.

739 Meta AI. Llama 3.2: Revolutionizing edge ai and vision with
 740 open, customizable models. <https://ai.meta.com/blog/llama-3-2-connect-2024-vision-edge-mobile-devices/>, 2024.

742 Soroush Nasiriany, Abhiram Maddukuri, Lance Zhang, Adeet Parikh, Aaron Lo, Abhishek Joshi,
 743 Ajay Mandlekar, and Yuke Zhu. Robocasa: Large-scale simulation of everyday tasks for generalist
 744 robots. *arXiv preprint arXiv:2406.02523*, 2024.

746 Liangbo Ning, Ziran Liang, Zhuohang Jiang, Haohao Qu, Yujuan Ding, Wenqi Fan, Xiao yong
 747 Wei, Shanru Lin, Hui Liu, Philip S. Yu, and Qing Li. A survey of webagents: Towards next-
 748 generation ai agents for web automation with large foundation models, 2025. URL <https://arxiv.org/abs/2503.23350>.

750 OpenAI. Gpt-4o system card, 2024. URL <https://arxiv.org/abs/2410.21276>.

751 Easton Potokar, Spencer Ashford, Michael Kaess, and Joshua G Mangelson. Holocean: An under-
 752 water robotics simulator. In *2022 International Conference on Robotics and Automation (ICRA)*,
 753 pp. 3040–3046. IEEE, 2022.

755 Archiki Prasad, Elias Stengel-Eskin, and Mohit Bansal. Rephrase, augment, reason: Visual ground-
 756 ing of questions for vision-language models. *arXiv preprint arXiv:2310.05861*, 2023.

756 Xavier Puig, Kevin Ra, Marko Boben, Jiaman Li, Tingwu Wang, Sanja Fidler, and Antonio Tor-
 757 ralba. Virtualhome: Simulating household activities via programs. In *Proceedings of the IEEE*
 758 *conference on computer vision and pattern recognition*, pp. 8494–8502, 2018.

759

760 Yanyuan Qiao, Haodong Hong, Wenqi Lyu, Dong An, Siqi Zhang, Yutong Xie, Xinyu Wang, and
 761 Qi Wu. Navbench: Probing multimodal large language models for embodied navigation, 2025.
 762 URL <https://arxiv.org/abs/2506.01031>.

763 Joseph Redmon, Santosh Kumar Divvala, Ross B. Girshick, and Ali Farhadi. You only look once:
 764 Unified, real-time object detection. In *2016 IEEE Conference on Computer Vision and Pattern*
 765 *Recognition, CVPR 2016, Las Vegas, NV, USA, June 27-30, 2016*, pp. 779–788. IEEE Computer
 766 Society, 2016. doi: 10.1109/CVPR.2016.91. URL <https://doi.org/10.1109/CVPR.2016.91>.

767

768 Cagatay Sariman, Ahmed Hallawa, and Anke Schmeink. Ur-earl: A framework for designing un-
 769 derwater robots using evolutionary algorithm-driven reinforcement learning. *Ocean Engineering*,
 770 321:120402, 2025.

771

772 Shital Shah, Debadatta Dey, Chris Lovett, and Ashish Kapoor. Airsim: High-fidelity visual and
 773 physical simulation for autonomous vehicles. In *Field and Service Robotics: Results of the 11th*
 774 *International Conference*, pp. 621–635. Springer, 2018.

775

776 Haochen Shi, Zhiyuan Sun, Xingdi Yuan, Marc-Alexandre Côté, and Bang Liu. OPEx: A
 777 component-wise analysis of LLM-centric agents in embodied instruction following. In Lun-Wei
 778 Ku, Andre Martins, and Vivek Srikanth (eds.), *Proceedings of the 62nd Annual Meeting of the As-*
 779 *sociation for Computational Linguistics (Volume 1: Long Papers)*, pp. 622–636, Bangkok, Thai-
 780 land, August 2024. Association for Computational Linguistics. doi: 10.18653/v1/2024.acl-long.
 37. URL <https://aclanthology.org/2024.acl-long.37>.

781

782 Fatemeh Shiri, Xiao-Yu Guo, Mona Far, Xin Yu, Reza Haf, and Yuan-Fang Li. An empirical anal-
 783 ysis on spatial reasoning capabilities of large multimodal models. In *Proceedings of the 2024*
 784 *Conference on Empirical Methods in Natural Language Processing, EMNLP 2024, Miami, FL,*
 785 *USA, November 12-16, 2024*, pp. 21440–21455. Association for Computational Linguistics, 2024.
 786 URL <https://aclanthology.org/2024.emnlp-main.1195>.

787

788 David Silver and Richard S Sutton. Welcome to the era of experience. *Google AI*, 1, 2025.

789

790 Jingyu Song, Haoyu Ma, Onur Bagoren, Advaith V. Sethuraman, Yiting Zhang, and Katherine A.
 791 Skinner. Oceansim: A gpu-accelerated underwater robot perception simulation framework, 2025.
 792 URL <https://arxiv.org/abs/2503.01074>.

793

794 Xinshuai Song, Weixing Chen, Yang Liu, Weikai Chen, Guanbin Li, and Liang Lin. Towards
 795 long-horizon vision-language navigation: Platform, benchmark and method. *arXiv preprint*
 796 *arXiv:2412.09082*, 2024.

797

798 Xiaoyu Tan, Bin Li, Xihe Qiu, Chao Qu, Wei Chu, Yinghui Xu, and Yuan Qi. Meta-agent-workflow:
 799 Streamlining tool usage in llms through workflow construction, retrieval, and refinement. In
 800 *Companion Proceedings of the ACM on Web Conference 2025, WWW '25*, pp. 458–467, New
 801 York, NY, USA, 2025. Association for Computing Machinery. ISBN 9798400713316. doi: 10.
 802 1145/3701716.3715247. URL <https://doi.org/10.1145/3701716.3715247>.

803

804 Xiangru Tang, Tianrui Qin, Tianhao Peng, Ziyang Zhou, Daniel Shao, Tingting Du, Ximeng Wei,
 805 Peng Xia, Fang Wu, He Zhu, Ge Zhang, Jiaheng Liu, Xingyao Wang, Sirui Hong, Chenglin Wu,
 806 Hao Cheng, Chi Wang, and Wangchunshu Zhou. Agent kb: Leveraging cross-domain experience
 807 for agentic problem solving, 2025. URL <https://arxiv.org/abs/2507.06229>.

808

809 V Team, Wenyi Hong, Wenmeng Yu, Xiaotao Gu, Guo Wang, Guobing Gan, Haomiao Tang, Jiale
 810 Cheng, Ji Qi, Junhui Ji, Lihang Pan, Shuaiqi Duan, Weihan Wang, Yan Wang, Yean Cheng, Zehai
 811 He, Zhe Su, Zhen Yang, Ziyang Pan, Aohan Zeng, Baoxu Wang, Bin Chen, Boyan Shi, Changyu
 812 Pang, Chenhui Zhang, Da Yin, Fan Yang, Guoqing Chen, Jiazheng Xu, Jiale Zhu, Jiali Chen,
 813 Jing Chen, Jinhao Chen, Jinghao Lin, Jinjiang Wang, Junjie Chen, Leqi Lei, Letian Gong, Leyi
 814 Pan, Mingdao Liu, Mingde Xu, Mingzhi Zhang, Qinkai Zheng, Sheng Yang, Shi Zhong, Shiyu

810 Huang, Shuyuan Zhao, Siyan Xue, Shangqin Tu, Shengbiao Meng, Tianshu Zhang, Tianwei Luo,
 811 Tianxiang Hao, Tianyu Tong, Wenkai Li, Wei Jia, Xiao Liu, Xiaohan Zhang, Xin Lyu, Xinyue Fan,
 812 Xuancheng Huang, Yanling Wang, Yadong Xue, Yanfeng Wang, Yanzi Wang, Yifan An, Yifan Du,
 813 Yiming Shi, Yiheng Huang, Yilin Niu, Yuan Wang, Yuanchang Yue, Yuchen Li, Yutao Zhang,
 814 Yuting Wang, Yu Wang, Yuxuan Zhang, Zhao Xue, Zhenyu Hou, Zhengxiao Du, Zihan Wang,
 815 Peng Zhang, Debing Liu, Bin Xu, Juanzi Li, Minlie Huang, Yuxiao Dong, and Jie Tang. Glm-
 816 4.5v and glm-4.1v-thinking: Towards versatile multimodal reasoning with scalable reinforcement
 817 learning, 2025. URL <https://arxiv.org/abs/2507.01006>.

818 Shengbang Tong, Zhuang Liu, Yuexiang Zhai, Yi Ma, Yann LeCun, and Saining Xie. Eyes wide
 819 shut? exploring the visual shortcomings of multimodal llms. In *IEEE/CVF Conference on Com-*
 820 *puter Vision and Pattern Recognition, CVPR 2024, Seattle, WA, USA, June 16-22, 2024*, pp. 9568–
 821 9578. IEEE, 2024. doi: 10.1109/CVPR52733.2024.00914. URL <https://doi.org/10.1109/CVPR52733.2024.00914>.

822 Hugo Touvron, Thibaut Lavril, Gautier Izacard, Xavier Martinet, Marie-Anne Lachaux, Timothée
 823 Lacroix, Baptiste Rozière, Naman Goyal, Eric Hambro, Faisal Azhar, Aurélien Rodriguez, Ar-
 824 mand Joulin, Edouard Grave, and Guillaume Lample. Llama: Open and efficient foun-
 825 dation language models. *CoRR*, abs/2302.13971, 2023. doi: 10.48550/arXiv.2302.13971. URL
 826 <https://doi.org/10.48550/arXiv.2302.13971>.

827 Arun Balajee Vasudevan, Dengxin Dai, and Luc Van Gool. Talk2nav: Long-range vision-and-
 828 language navigation with dual attention and spatial memory. *International Journal of Computer
 829 Vision*, 129(1):246–266, 2021.

830 Martin Visbeck. Ocean science research is key for a sustainable future. *Nature communications*, 9
 831 (1):690, 2018.

832 Chen Wang, Fei Xia, Wenhao Yu, Tingnan Zhang, Ruohan Zhang, C. Karen Liu, Li Fei-Fei, Jie
 833 Tan, and Jacky Liang. Chain-of-modality: Learning manipulation programs from multimodal hu-
 834 man videos with vision-language-models, 2025a. URL <https://arxiv.org/abs/2504.13351>.

835 Weiyun Wang, Zhangwei Gao, Lixin Gu, Hengjun Pu, Long Cui, Xinguang Wei, Zhaoyang
 836 Liu, Linglin Jing, Shenglong Ye, Jie Shao, Zhaokai Wang, Zhe Chen, Hongjie Zhang, Ganlin
 837 Yang, Haomin Wang, Qi Wei, Jinhui Yin, Wenhao Li, Erfei Cui, Guanzhou Chen, Zichen Ding,
 838 Changyao Tian, Zhenyu Wu, Jingjing Xie, Zehao Li, Bowen Yang, Yuchen Duan, Xuehui Wang,
 839 Zhi Hou, Haoran Hao, Tianyi Zhang, Songze Li, Xiangyu Zhao, Haodong Duan, Nianchen Deng,
 840 Bin Fu, Yinan He, Yi Wang, Conghui He, Botian Shi, Junjun He, Yingtong Xiong, Han Lv, Lijun
 841 Wu, Wenqi Shao, Kaipeng Zhang, Huipeng Deng, Biqing Qi, Jiaye Ge, Qipeng Guo, Wenwei
 842 Zhang, Songyang Zhang, Maosong Cao, Junyao Lin, Kexian Tang, Jianfei Gao, Haian Huang,
 843 Yuzhe Gu, Chengqi Lyu, Huanze Tang, Rui Wang, Haijun Lv, Wanli Ouyang, Limin Wang, Min
 844 Dou, Xizhou Zhu, Tong Lu, Dahua Lin, Jifeng Dai, Weijie Su, Bowen Zhou, Kai Chen, Yu Qiao,
 845 Weihai Wang, and Gen Luo. Internvl3.5: Advancing open-source multimodal models in versatil-
 846 ity, reasoning, and efficiency, 2025b. URL <https://arxiv.org/abs/2508.18265>.

847 Xiangyu Wang, Donglin Yang, Ziqin Wang, Hohin Kwan, Jinyu Chen, Wenjun Wu, Hongsheng Li,
 848 Yue Liao, and Si Liu. Towards realistic uav vision-language navigation: Platform, benchmark,
 849 and methodology, 2024a. URL <https://arxiv.org/abs/2410.07087>.

850 Xiangyu Wang, Donglin Yang, Ziqin Wang, Hohin Kwan, Jinyu Chen, Wenjun Wu, Hongsheng Li,
 851 Yue Liao, and Si Liu. Towards realistic uav vision-language navigation: Platform, benchmark,
 852 and methodology, 2024b. URL <https://arxiv.org/abs/2410.07087>.

853 Di Wu, Hongwei Wang, Wenhao Yu, Yuwei Zhang, Kai-Wei Chang, and Dong Yu. Longmemeval:
 854 Benchmarking chat assistants on long-term interactive memory, 2024.

855 Yi Wu, Yuxin Wu, Georgia Gkioxari, and Yuandong Tian. Building generalizable agents with a
 856 realistic and rich 3d environment, 2018. URL <https://openreview.net/forum?id=rkaT3zWCZ>.

864 Zhiheng Xi, Wenxiang Chen, Xin Guo, Wei He, Yiwen Ding, Boyang Hong, Ming Zhang, Jun-
 865 zhe Wang, Senjie Jin, Enyu Zhou, Rui Zheng, Xiaoran Fan, Xiao Wang, Limao Xiong, Yuhao
 866 Zhou, Weiran Wang, Changhao Jiang, Yicheng Zou, Xiangyang Liu, Zhangyue Yin, Shihan Dou,
 867 Rongxiang Weng, Wenjuan Qin, Yongyan Zheng, Xipeng Qiu, Xuanjing Huang, Qi Zhang, and
 868 Tao Gui. The rise and potential of large language model based agents: a survey. *Sci. China Inf.
 869 Sci.*, 68(2), 2025. doi: 10.1007/S11432-024-4222-0. URL <https://doi.org/10.1007/s11432-024-4222-0>.

870

871 Fanbo Xiang, Yuzhe Qin, Kaichun Mo, Yikuan Xia, Hao Zhu, Fangchen Liu, Minghua Liu, Hanxiao
 872 Jiang, Yifu Yuan, He Wang, et al. Sapien: A simulated part-based interactive environment. In
 873 *Proceedings of the IEEE/CVF conference on computer vision and pattern recognition*, pp. 11097–
 874 11107, 2020.

875

876 Kaibing Xie, Jian Yang, and Kang Qiu. A dataset with multibeam forward-looking sonar for under-
 877 water object detection. *CoRR*, abs/2212.00352, 2022. doi: 10.48550/ARXIV.2212.00352. URL
 878 <https://doi.org/10.48550/arXiv.2212.00352>.

879

880 Wei Xu, Cheng Wang, Dingkang Liang, Zongchuang Zhao, Xingyu Jiang, Peng Zhang, and Xi-
 881 ang Bai. Nautilus: A large multimodal model for underwater scene understanding, 2025. URL
 882 <https://arxiv.org/abs/2510.27481>.

883

884 An Yang, Anfeng Li, Baosong Yang, Beichen Zhang, Binyuan Hui, Bo Zheng, Bowen Yu, Chang
 885 Gao, Chengan Huang, Chenxu Lv, Chujie Zheng, Dayiheng Liu, Fan Zhou, Fei Huang, Feng
 886 Hu, Hao Ge, Haoran Wei, Huan Lin, Jialong Tang, Jian Yang, Jianhong Tu, Jianwei Zhang,
 887 Jian Yang, Jiaxi Yang, Jingren Zhou, Junyang Lin, Kai Dang, Keqin Bao, Kexin Yang, Le Yu,
 888 Lianghao Deng, Mei Li, Mingfeng Xue, Mingze Li, Pei Zhang, Peng Wang, Qin Zhu, Rui Men,
 889 Ruize Gao, Shixuan Liu, Shuang Luo, Tianhao Li, Tianyi Tang, Wenbiao Yin, Xingzhang Ren,
 890 Xinyu Wang, Xinyu Zhang, Xuancheng Ren, Yang Fan, Yang Su, Yichang Zhang, Yingger Zhang,
 891 Yu Wan, Yuqiong Liu, Zekun Wang, Zeyu Cui, Zhenru Zhang, Zhipeng Zhou, and Zihan Qiu.
 892 Qwen3 technical report. *CoRR*, abs/2505.09388, 2025a. doi: 10.48550/ARXIV.2505.09388. URL
 893 <https://doi.org/10.48550/arXiv.2505.09388>.

894

895 Rui Yang, Hanyang Chen, Junyu Zhang, Mark Zhao, Cheng Qian, Kangrui Wang, Qineng Wang,
 896 Teja Venkat Koripella, Marziyeh Movahedi, Manling Li, Heng Ji, Huan Zhang, and Tong Zhang.
 897 Embodiedbench: Comprehensive benchmarking multi-modal large language models for vision-
 898 driven embodied agents, 2025b. URL <https://arxiv.org/abs/2502.09560>.

899

900 Sihan Yang, Runsen Xu, Yiman Xie, Sizhe Yang, Mo Li, Jingli Lin, Chenming Zhu, Xiaochen
 901 Chen, Haodong Duan, Xiangyu Yue, Dahua Lin, Tai Wang, and Jiangmiao Pang. Mmsi-bench:
 902 A benchmark for multi-image spatial intelligence, 2025c. URL <https://arxiv.org/abs/2505.23764>.

903

904 Fanglong Yao, Yuanchang Yue, Youzhi Liu, Xian Sun, and Kun Fu. Aeroverse: Uav-agent bench-
 905 mark suite for simulating, pre-training, finetuning, and evaluating aerospace embodied world
 906 models. *CoRR*, abs/2408.15511, 2024. doi: 10.48550/ARXIV.2408.15511. URL <https://doi.org/10.48550/arXiv.2408.15511>.

907

908 Yuan Yao, Tianyu Yu, Ao Zhang, Chongyi Wang, Junbo Cui, Hongji Zhu, Tianchi Cai, Haoyu Li,
 909 Weilin Zhao, Zhihui He, et al. Minicpm-v: A gpt-4v level mllm on your phone. *Nat Commun* 16,
 910 5509 (2025), 2025.

911

912 Qiyuan Zhang, Fuyuan Lyu, Zexu Sun, Lei Wang, Weixu Zhang, Zhihan Guo, Yufei Wang, Irwin
 913 King, Xue Liu, and Chen Ma. What, how, where, and how well? A survey on test-time scaling in
 914 large language models. *CoRR*, abs/2503.24235, 2025a. doi: 10.48550/ARXIV.2503.24235. URL
 915 <https://doi.org/10.48550/arXiv.2503.24235>.

916

917 Yifan Zhang, Huanyu Zhang, Haochen Tian, Chaoyou Fu, Shuangqing Zhang, Junfei Wu, Feng Li,
 918 Kun Wang, Qingsong Wen, Zhang Zhang, Liang Wang, and Rong Jin. Mme-realworld: Could
 919 your multimodal LLM challenge high-resolution real-world scenarios that are difficult for hu-
 920 mans? In *The Thirteenth International Conference on Learning Representations, ICLR 2025,
 921 Singapore, April 24-28, 2025*. OpenReview.net, 2025b. URL <https://openreview.net/forum?id=k5VHHgsRbi>.

918 Baining Zhao, Jianjie Fang, Zichao Dai, Ziyou Wang, Jirong Zha, Weichen Zhang, Chen Gao,
 919 Yue Wang, Jinqiang Cui, Xinlei Chen, and Yong Li. Urbanvideo-bench: Benchmarking vision-
 920 language models on embodied intelligence with video data in urban spaces, 2025. URL <https://arxiv.org/abs/2503.06157>.

921 Wayne Xin Zhao, Kun Zhou, Junyi Li, Tianyi Tang, Xiaolei Wang, Yupeng Hou, Yingqian Min,
 923 Beichen Zhang, Junjie Zhang, Zican Dong, et al. A survey of large language models. *arXiv*
 924 *preprint arXiv:2303.18223*, 1(2), 2023.

925 Kaizhi Zheng, Xiaotong Chen, Odest Chadwicke Jenkins, and Xin Wang. Vlmbench: A composi-
 926 tional benchmark for vision-and-language manipulation. *Advances in Neural Information Pro-*
 927 *cessing Systems*, 35:665–678, 2022a.

928 Kaizhi Zheng, Xiaotong Chen, Odest Chadwicke Jenkins, and Xin Wang. Vlmbench: A composi-
 929 tional benchmark for vision-and-language manipulation. *Advances in Neural Information Pro-*
 930 *cessing Systems*, 35:665–678, 2022b.

931 Kening Zheng, Junkai Chen, Yibo Yan, Xin Zou, and Xuming Hu. Reefknot: A comprehensive
 932 benchmark for relation hallucination evaluation, analysis and mitigation in multimodal large
 933 language models. *CoRR*, abs/2408.09429, 2024. doi: 10.48550/ARXIV.2408.09429. URL
 934 <https://doi.org/10.48550/arXiv.2408.09429>.

935 Ziqiang Zheng, Jipeng Zhang, Tuan-Anh Vu, Shizhe Diao, Yue Him Wong Tim, and Sai-Kit Yeung.
 936 Marinegpt: Unlocking secrets of ocean to the public. *arXiv preprint arXiv:2310.13596*, 2023.

937 Wanjun Zhong, Lianghong Guo, Qiqi Gao, He Ye, and Yanlin Wang. Memorybank: Enhancing large
 938 language models with long-term memory. In *Proceedings of the AAAI Conference on Artificial*
 939 *Intelligence*, 2024.

940 Gengze Zhou, Yicong Hong, and Qi Wu. Navgpt: Explicit reasoning in vision-and-language naviga-
 941 tion with large language models. In *Proceedings of the AAAI Conference on Artificial Intelligence*,
 942 volume 38, pp. 7641–7649, 2024a.

943 Qinrong Zhou, Sunli Chen, Yisong Wang, Haozhe Xu, Weihua Du, Hongxin Zhang, Yilun Du,
 944 Joshua B. Tenenbaum, and Chuang Gan. HAZARD challenge: Embodied decision making
 945 in dynamically changing environments. In *The Twelfth International Conference on Learning*
 946 *Representations, ICLR 2024, Vienna, Austria, May 7-11, 2024*. OpenReview.net, 2024b. URL
 947 <https://openreview.net/forum?id=n6mLhaBahJ>.

948 King Zhu, Hanhao Li, Siwei Wu, Tianshun Xing, Dehua Ma, Xiangru Tang, Minghao Liu, Jian Yang,
 949 Jiaheng Liu, Yuchen Eleanor Jiang, Changwang Zhang, Chenghua Lin, Jun Wang, Ge Zhang, and
 950 Wangchunshu Zhou. Scaling test-time compute for LLM agents. *CoRR*, abs/2506.12928, 2025.
 951 doi: 10.48550/ARXIV.2506.12928. URL <https://doi.org/10.48550/arXiv.2506.12928>.

952
 953
 954
 955
 956
 957
 958
 959
 960
 961
 962
 963
 964
 965
 966
 967
 968
 969
 970
 971

972 A APPENDIX

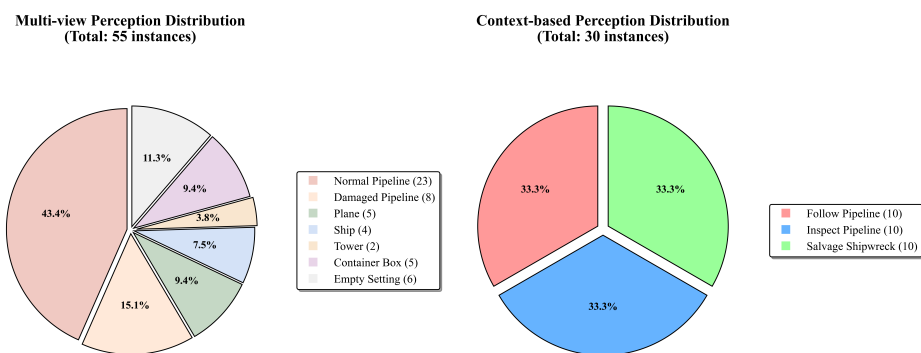
974 A.1 THE USE OF LARGE LANGUAGE MODELS (LLMs)

976 We confirm that LLMs are used only as an auxiliary tool to assist in refining wording and sentence
 977 structure. Their application in experiments is strictly confined to scientific research purposes, and
 978 all such uses have been clearly documented in the Experimental Settings. No additional reliance on
 979 LLMs has been involved in this work.

981 A.2 MORE DETAILED DISCUSSES AND LIMITATIONS

983 **Limitations.** While OCEANGYM provides a valuable testbed for underwater embodied agents, sev-
 984 eral limitations should be acknowledged. First, OceanGym leverages Unreal Engine (UE) 5.3 (Epic
 985 Games, 2025) for realistic underwater environment rendering and physical simulation, while uti-
 986 lizing HoloOcean’s (Potokar et al., 2022) cluster-based multipath ray-tracing algorithm to simulate
 987 multibeam sonar. Although UE plugins can be used to simulate water flow, buoyancy, lighting, water
 988 interaction etc, it cannot fully replicate the real underwater environment, as factors such as ocean
 989 currents, salinity, marine life, and geological changes are not accurately captured. Future work may
 990 leverage generative models (Ball et al., 2025) or physics-informed machine learning to incorporate
 991 these complexities. The optical and sonar images still differ from those in the real world, particu-
 992 larly since sonar simulation introduces errors. We will continue to refine the system to reduce these
 993 discrepancies, noting that real-world sonar itself is also subject to noise and inaccuracies. In addi-
 994 tion, the environment is large and requires considerable computational resources, with at least 24GB
 995 of GPU memory. We recommend running without a graphical interface, as enabling it can cause
 996 significant lag. These limitations highlight opportunities for future work to expand task coverage,
 997 improve physical realism, and optimize computational efficiency.

998 **Applications of OceanGym.** (1) A competitive arena for evaluating foundational models and em-
 999 bodied agent frameworks, particularly memory mechanisms. Future work can leverage OCEANGYM
 1000 to optimize prompt design, memory utilization, and base model capabilities. (2) A platform for
 1001 synthesizing underwater simulation data to enhance both perception and decision-making skills of
 1002 agents. (3) A testbed for reinforcement learning, providing rich feedback for training autonomous
 1003 behaviors. (4) A sim-to-real bridge, enabling the transfer of trained models to real-world AUVs.
 1004 By connecting virtual training with real-world deployment, OCEANGYM substantially reduces de-
 1005 pendence on costly and hazardous field trials, accelerates development cycles, and enhances the
 1006 reliability and robustness of autonomous underwater systems.



1019 Figure 9: Statistics of perception tasks.

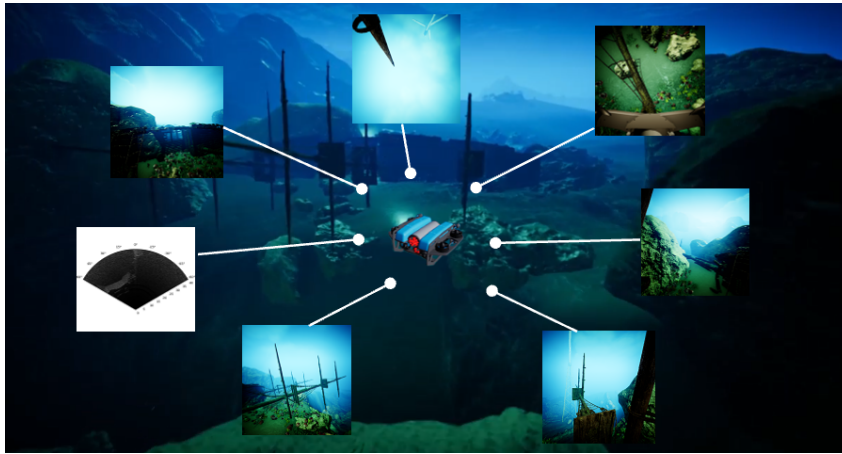
1021 A.3 PERCEPTION TASK STATISTICS

1023 Figure 9 presents the statistical distribution of different perception settings analyzed in our dataset.
 1024 The dataset consists of 85 sets of data, which include 55 sets focusing on Multi-view Perception and
 1025 30 sets on Context-based Perception. Within the Multi-view Perception data, 55 sets are categorized
 as follows: 23 sets involve normal pipelines, 8 sets entail damaged pipelines, 5 sets are related to

1026 planes, 4 sets concern ships, 2 sets focus on towers, 5 sets involve container boxes, and 6 sets do not
 1027 feature any specific dominant object. For the Context-based Perception data, the 30 sets are evenly
 1028 divided among three distinct sub-tasks, each comprising 10 sets. These sub-tasks involve the agent
 1029 following pipelines, inspecting pipelines for potential damage, and scanning around shipwrecks.
 1030

1031 A.4 DECISION TASK DETAILS

1032
 1033 Decision-making tasks require an embodied agent to accomplish a given objective through a series
 1034 of decisions. Figure 10 illustrates the perceptual input at one specific state during such a task.
 1035



1036
 1037
 1038
 1039
 1040
 1041
 1042
 1043
 1044
 1045
 1046
 1047
 1048
 1049
 1050
 1051
 1052
 1053
 1054
 1055
 1056
 1057
 1058
 1059
 1060
 1061
 1062
 1063
 1064
 1065
 1066
 1067
 1068
 1069
 1070
 1071
 1072
 1073
 1074
 1075
 1076
 1077
 1078
 1079
 1080
 1081
 1082
 1083
 1084
 1085
 1086
 1087
 1088
 1089
 1090
 1091
 1092
 1093
 1094
 1095
 1096
 1097
 1098
 1099
 1100
 1101
 1102
 1103
 1104
 1105
 1106
 1107
 1108
 1109
 1110
 1111
 1112
 1113
 1114
 1115
 1116
 1117
 1118
 1119
 1120
 1121
 1122
 1123
 1124
 1125
 1126
 1127
 1128
 1129
 1130
 1131
 1132
 1133
 1134
 1135
 1136
 1137
 1138
 1139
 1140
 1141
 1142
 1143
 1144
 1145
 1146
 1147
 1148
 1149
 1150
 1151
 1152
 1153
 1154
 1155
 1156
 1157
 1158
 1159
 1160
 1161
 1162
 1163
 1164
 1165
 1166
 1167
 1168
 1169
 1170
 1171
 1172
 1173
 1174
 1175
 1176
 1177
 1178
 1179
 1180
 1181
 1182
 1183
 1184
 1185
 1186
 1187
 1188
 1189
 1190
 1191
 1192
 1193
 1194
 1195
 1196
 1197
 1198
 1199
 1200
 1201
 1202
 1203
 1204
 1205
 1206
 1207
 1208
 1209
 1210
 1211
 1212
 1213
 1214
 1215
 1216
 1217
 1218
 1219
 1220
 1221
 1222
 1223
 1224
 1225
 1226
 1227
 1228
 1229
 1230
 1231
 1232
 1233
 1234
 1235
 1236
 1237
 1238
 1239
 1240
 1241
 1242
 1243
 1244
 1245
 1246
 1247
 1248
 1249
 1250
 1251
 1252
 1253
 1254
 1255
 1256
 1257
 1258
 1259
 1260
 1261
 1262
 1263
 1264
 1265
 1266
 1267
 1268
 1269
 1270
 1271
 1272
 1273
 1274
 1275
 1276
 1277
 1278
 1279
 1280
 1281
 1282
 1283
 1284
 1285
 1286
 1287
 1288
 1289
 1290
 1291
 1292
 1293
 1294
 1295
 1296
 1297
 1298
 1299
 1300
 1301
 1302
 1303
 1304
 1305
 1306
 1307
 1308
 1309
 1310
 1311
 1312
 1313
 1314
 1315
 1316
 1317
 1318
 1319
 1320
 1321
 1322
 1323
 1324
 1325
 1326
 1327
 1328
 1329
 1330
 1331
 1332
 1333
 1334
 1335
 1336
 1337
 1338
 1339
 1340
 1341
 1342
 1343
 1344
 1345
 1346
 1347
 1348
 1349
 1350
 1351
 1352
 1353
 1354
 1355
 1356
 1357
 1358
 1359
 1360
 1361
 1362
 1363
 1364
 1365
 1366
 1367
 1368
 1369
 1370
 1371
 1372
 1373
 1374
 1375
 1376
 1377
 1378
 1379
 1380
 1381
 1382
 1383
 1384
 1385
 1386
 1387
 1388
 1389
 1390
 1391
 1392
 1393
 1394
 1395
 1396
 1397
 1398
 1399
 1400
 1401
 1402
 1403
 1404
 1405
 1406
 1407
 1408
 1409
 1410
 1411
 1412
 1413
 1414
 1415
 1416
 1417
 1418
 1419
 1420
 1421
 1422
 1423
 1424
 1425
 1426
 1427
 1428
 1429
 1430
 1431
 1432
 1433
 1434
 1435
 1436
 1437
 1438
 1439
 1440
 1441
 1442
 1443
 1444
 1445
 1446
 1447
 1448
 1449
 1450
 1451
 1452
 1453
 1454
 1455
 1456
 1457
 1458
 1459
 1460
 1461
 1462
 1463
 1464
 1465
 1466
 1467
 1468
 1469
 1470
 1471
 1472
 1473
 1474
 1475
 1476
 1477
 1478
 1479
 1480
 1481
 1482
 1483
 1484
 1485
 1486
 1487
 1488
 1489
 1490
 1491
 1492
 1493
 1494
 1495
 1496
 1497
 1498
 1499
 1500
 1501
 1502
 1503
 1504
 1505
 1506
 1507
 1508
 1509
 1510
 1511
 1512
 1513
 1514
 1515
 1516
 1517
 1518
 1519
 1520
 1521
 1522
 1523
 1524
 1525
 1526
 1527
 1528
 1529
 1530
 1531
 1532
 1533
 1534
 1535
 1536
 1537
 1538
 1539
 1540
 1541
 1542
 1543
 1544
 1545
 1546
 1547
 1548
 1549
 1550
 1551
 1552
 1553
 1554
 1555
 1556
 1557
 1558
 1559
 1560
 1561
 1562
 1563
 1564
 1565
 1566
 1567
 1568
 1569
 1570
 1571
 1572
 1573
 1574
 1575
 1576
 1577
 1578
 1579
 1580
 1581
 1582
 1583
 1584
 1585
 1586
 1587
 1588
 1589
 1590
 1591
 1592
 1593
 1594
 1595
 1596
 1597
 1598
 1599
 1600
 1601
 1602
 1603
 1604
 1605
 1606
 1607
 1608
 1609
 1610
 1611
 1612
 1613
 1614
 1615
 1616
 1617
 1618
 1619
 1620
 1621
 1622
 1623
 1624
 1625
 1626
 1627
 1628
 1629
 1630
 1631
 1632
 1633
 1634
 1635
 1636
 1637
 1638
 1639
 1640
 1641
 1642
 1643
 1644
 1645
 1646
 1647
 1648
 1649
 1650
 1651
 1652
 1653
 1654
 1655
 1656
 1657
 1658
 1659
 1660
 1661
 1662
 1663
 1664
 1665
 1666
 1667
 1668
 1669
 1670
 1671
 1672
 1673
 1674
 1675
 1676
 1677
 1678
 1679
 1680
 1681
 1682
 1683
 1684
 1685
 1686
 1687
 1688
 1689
 1690
 1691
 1692
 1693
 1694
 1695
 1696
 1697
 1698
 1699
 1700
 1701
 1702
 1703
 1704
 1705
 1706
 1707
 1708
 1709
 1710
 1711
 1712
 1713
 1714
 1715
 1716
 1717
 1718
 1719
 1720
 1721
 1722
 1723
 1724
 1725
 1726
 1727
 1728
 1729
 1730
 1731
 1732
 1733
 1734
 1735
 1736
 1737
 1738
 1739
 1740
 1741
 1742
 1743
 1744
 1745
 1746
 1747
 1748
 1749
 1750
 1751
 1752
 1753
 1754
 1755
 1756
 1757
 1758
 1759
 1760
 1761
 1762
 1763
 1764
 1765
 1766
 1767
 1768
 1769
 1770
 1771
 1772
 1773
 1774
 1775
 1776
 1777
 1778
 1779
 1780
 1781
 1782
 1783
 1784
 1785
 1786
 1787
 1788
 1789
 1790
 1791
 1792
 1793
 1794
 1795
 1796
 1797
 1798
 1799
 1800
 1801
 1802
 1803
 1804
 1805
 1806
 1807
 1808
 1809
 1810
 1811
 1812
 1813
 1814
 1815
 1816
 1817
 1818
 1819
 1820
 1821
 1822
 1823
 1824
 1825
 1826
 1827
 1828
 1829
 1830
 1831
 1832
 1833
 1834
 1835
 1836
 1837
 1838
 1839
 1840
 1841
 1842
 1843
 1844
 1845
 1846
 1847
 1848
 1849
 1850
 1851
 1852
 1853
 1854
 1855
 1856
 1857
 1858
 1859
 1860
 1861
 1862
 1863
 1864
 1865
 1866
 1867
 1868
 1869
 1870
 1871
 1872
 1873
 1874
 1875
 1876
 1877
 1878
 1879
 1880
 1881
 1882
 1883
 1884
 1885
 1886
 1887
 1888
 1889
 1890
 1891
 1892
 1893
 1894
 1895
 1896
 1897
 1898
 1899
 1900
 1901
 1902
 1903
 1904
 1905
 1906
 1907
 1908
 1909
 1910
 1911
 1912
 1913
 1914
 1915
 1916
 1917
 1918
 1919
 1920
 1921
 1922
 1923
 1924
 1925
 1926
 1927
 1928
 1929
 1930
 1931
 1932
 1933
 1934
 1935
 1936
 1937
 1938
 1939
 1940
 1941
 1942
 1943
 1944
 1945
 1946
 1947
 1948
 1949
 1950
 1951
 1952
 1953
 1954
 1955
 1956
 1957
 1958
 1959
 1960
 1961
 1962
 1963
 1964
 1965
 1966
 1967
 1968
 1969
 1970
 1971
 1972
 1973
 1974
 1975
 1976
 1977
 1978
 1979
 1980
 1981
 1982
 1983
 1984
 1985
 1986
 1987
 1988
 1989
 1990
 1991
 1992
 1993
 1994
 1995
 1996
 1997
 1998
 1999
 2000
 2001
 2002
 2003
 2004
 2005
 2006
 2007
 2008
 2009
 2010
 2011
 2012
 2013
 2014
 2015
 2016
 2017
 2018
 2019
 2020
 2021
 2022
 2023
 2024
 2025
 2026
 2027
 2028
 2029
 2030
 2031
 2032
 2033
 2034
 2035
 2036
 2037
 2038
 2039
 2040
 2041
 2042
 2043
 2044
 2045
 2046
 2047
 2048
 2049
 2050
 2051
 2052
 2053
 2054
 2055
 2056
 2057
 2058
 2059
 2060
 2061
 2062
 2063
 2064
 2065
 2066
 2067
 2068
 2069
 2070
 2071
 2072
 2073
 2074
 2075
 2076
 2077
 2078
 2079
 2080
 2081
 2082
 2083
 2084
 2085
 2086
 2087
 2088
 2089
 2090
 2091
 2092
 2093
 2094
 2095
 2096
 2097
 2098
 2099
 2100
 2101
 2102
 2103
 2104
 2105
 2106
 2107
 2108
 2109
 2110
 2111
 2112
 2113
 2114
 2115
 2116
 2117
 2118
 2119
 2120
 2121
 2122
 2123
 2124
 2125
 2126
 2127
 2128
 2129
 2130
 2131
 2132
 2133
 2134
 2135
 2136
 2137
 2138
 2139
 2140
 2141
 2142
 2143
 2144
 2145
 2146
 2147
 2148
 2149
 2150
 2151
 2152
 2153
 2154
 2155
 2156
 2157
 2158
 2159
 2160
 2161
 2162
 2163
 2164
 2165
 2166
 2167
 2168
 2169
 2170
 2171
 2172
 2173
 2174
 2175
 2176
 2177
 2178
 2179
 2180
 2181
 2182
 2183
 2184
 2185
 2186
 2187
 2188
 2189
 2190
 2191
 2192
 2193
 2194
 2195
 2196
 2197
 2198
 2199
 2200
 2201
 2202
 2203
 2204
 2205
 2206
 2207
 2208
 2209
 2210
 2211
 2212
 2213
 2214
 2215
 2216
 2217
 2218
 2219
 2220
 2221
 2222
 2223
 2224
 2225
 2226
 2227
 2228
 2229
 2230
 2231
 2232
 2233
 2234
 2235
 2236
 2237
 2238
 2239
 2240
 2241
 2242
 2243
 2244
 2245
 2246
 2247
 2248
 2249
 2250
 2251
 2252
 2253
 2254
 2255
 2256
 2257
 2258
 2259
 2260
 2261
 2262
 2263
 2264
 2265
 2266
 2267
 2268
 2269
 2270
 2271
 2272
 2273
 2274
 2275
 2276
 2277
 2278
 2279
 2280
 2281
 2282
 2283
 2284
 2285
 2286
 2287
 2288
 2289
 2290
 2291
 2292
 2293
 2294
 2295
 2296
 2297
 2298
 2299
 2300
 2301
 2302
 2303
 2304
 2305
 2306
 2307
 2308
 2309
 2310
 2311
 2312
 2313
 2314
 2315
 2316
 2317
 2318
 2319
 2320
 2321
 2322
 2323
 2324
 2325
 2326
 2327
 2328
 2329
 2330
 2331
 2332
 2333
 2334
 2335
 2336
 2337
 2338
 2339
 2340
 2341
 2342
 2343
 2344
 2345
 2346
 2347
 2348
 2349
 2350
 2351
 2352
 2353
 2354
 2355
 2356
 2357
 2358
 2359
 2360
 2361
 2362
 2363
 2364
 2365
 2366
 2367
 2368
 2369
 2370
 2371
 2372
 2373
 2374
 2375
 2376
 2377
 2378
 2379
 2380
 2381
 2382
 2383
 2384
 2385
 2386
 2387
 2388
 2389
 2390
 2391
 2392
 2393
 2394
 2395
 2396
 2397
 2398
 2399
 240



1080
1081
1082
1083
1084
1085
1086
1087
1088
1089
1090
1091
1092
1093
1094
1095
1096
1097
1098
1099
1100
1101
1102
1103
1104
1105
1106
1107
1108
1109
1110
1111
1112
1113
1114
1115
1116
1117
1118
1119
1120
1121
1122
1123
1124
1125
1126
1127
1128
1129
1130
1131
1132
1133
Figure 11: Target object for the “Locate the robot” task.



Figure 12: Target object for the “Inspect the oil pipe” task.



Figure 13: Target object for the “Locate oil drums” task.



Figure 14: Target object for the “Search for a sunken ship” task.



Figure 15: Target object for the “Locate the electrical box” task.



Figure 16: Target object for the “Inspect the wind turbine” task.



Figure 17: Target object for the “Search for the aircraft” task.



Figure 18: Target object for the “Docking” task.

Search for a sunken ship. Locate and identify sunken shipwrecks, which are typically structurally complex entities that may be partially buried or obscured by various underwater obstacles. The mission initiates with an access of the robot’s memory for any known coordinates of shipwrecks, utilizing them for direct navigation if available. In the absence of positional data, the robot relies on its camera feeds to recognize large structural features and surface details that correspond to the reference images of a shipwreck. A systematic exploration is subsequently performed to document all special objects within the area. A safe distance from all obstacles must be maintained throughout the operation, and the vehicle is required to stay within its prescribed operational limits. All marine life is systematically ignored and excluded from reporting.

Locate the electrical box. Locate and identify underwater electrical boxes, which are often partially buried in sediment and possess distinctive structural features. The operational sequence starts with a retrieval attempt from the robot’s memory for the coordinates of electrical boxes, followed by direct navigation to any located waypoints. Without prior coordinate data, the robot must analyze its camera feeds to identify the target based on its specific shape, structural characteristics, and any identifiable markings. A thorough and systematic exploration of the zone is then carried out, with all special objects recorded. The mission must adhere to strict obstacle avoidance procedures and remain within the defined operational boundaries at all times. All communications and reports are restricted to artificial structures and special objects.

Inspect the wind turbine. Locate and identify underwater wind power station structures, which are large installations featuring multiple pillars and mechanical components. The robot first searches its internal memory for stored coordinates of the wind power station, navigating directly to the location if the data is found. If the coordinates are not located, the system uses its camera arrays to identify the major structural and mechanical elements that match the reference documentation. A systematic exploration pattern is executed to document every special object in the vicinity. A safe buffer distance from all obstacles is perpetually maintained, and the robot’s path must comply strictly with the operational boundaries. Any biological entities encountered are disregarded and not included in any reports.

Search for the aircraft. Locate and identify underwater aircraft wreckage, which can be complex and potentially dispersed across different areas of the seafloor. The initial phase involves a memory check for any existing coordinates related to aircraft wreckage, with immediate navigation initiated upon a successful find. If no data is available, the robot switches to using its visual feeds to identify key structural features and surface details that are consistent with the target wreckage. A comprehensive systematic search is then conducted, ensuring all special objects are documented. Strict obstacle avoidance is paramount, and the vehicle must operate entirely within the set boundaries. Reports are exclusively to contain information on artificial structures and special objects.

1134 **Docking.** Locate and identify an underwater landing platform marked with a distinctive "H" symbol.
 1135 a structure with a regular form that provides a reliable navigation reference. The robot's first
 1136 action is to consult its memory for the platform's coordinates, proceeding with direct navigation
 1137 if the information is available. Should the coordinates be absent, the platform must be identified
 1138 visually through the camera feeds by recognizing the "H" marking and the overall platform struc-
 1139 ture. This is followed by a systematic exploration to document all special objects in the area. A
 1140 safe distance from all obstacles must be maintained, and the operation is confined to the approved
 1141 boundaries. All reporting is limited to artificial structures and special objects, with no mention of
 1142 biological activity.

1143

1144 A.5 PROMPT FOR OCEANGYM

1145

1146 Prompt for Perception Tasks

1147

1148 **[RGB Image]**1149 You are an assistant that analyzes an image and checks which of the following options appear
 1150 in it.

1151

1152 Options:**[Options]**

1153 Instructions:

1154

1155 - Carefully examine the image, even the corners.

1156

1157 - You can choose single or multiple options, if none of the options appear, just return an
 1158 empty list.

1159

1160 - For multiple-choice questions, no points will be awarded for incomplete selections, over-
 1161 selections, or incorrect selections.

1162

1163 - The output must be a valid list (only list, no explanation, no extra text).

1164

1165 Prompt for Perception Tasks (Add Sonar)

1166

1167 **[Sonar Image]**

1168 This sonar image can be used as a reference to assist in identifying the next color image.

1169

1170 **[RGB Image]**1171 You are an assistant that analyzes an image and checks which of the following options appear
 1172 in it. Before that, I have already provide you a sonar image to help you choose the correct
 1173 one.

1174

1175 Options:**[Options]**

1176 Instructions:

1177

1178 - Only when you find it difficult to recognize the color image, I suggest you refer to the
 1179 previous sonar image together.

1180

1181 - Carefully examine the image, even the corners.

1182

1183 - You can choose single or multiple options, if none of the options appear, just return an
 1184 empty list.

1185

1186 - For multiple-choice questions, no points will be awarded for incomplete selections, over-
 1187 selections, or incorrect selections.

1188

1189 - The output must be a valid list (only list, no explanation, no extra text).

1190

1191 Prompt for Perception Tasks (Add Sonar and Examples)

1192

1193 **[Object A Sonar Image]**1194 This sonar image example is **[Object A]**.

1195

1196 **[Object B Sonar Image]**1197 This sonar image example is **[Object B]**.

1198

1199 ...

1200

1201 **[Sonar Image]**

1188

1189 This sonar image can be used as a reference to assist in identifying the next color image.

1190

1191 **[RGB Image]**1192 You are an assistant that analyzes an image and checks which of the following options appear
1193 in it. Before that, I have already provide you a sonar image to help you choose the correct
1194 one.1195 Options:**[Options]**

1196 Instructions:

1197

- Only when you find it difficult to recognize the color image, I suggest you refer to the
1198 previous sonar image together.
- Carefully examine the image, even the corners.
- You can choose single or multiple options, if none of the options appear, just return an
1200 empty list.
- For multiple-choice questions, no points will be awarded for incomplete selections, over-
1202 selections, or incorrect selections.
- The output must be a valid list (only list, no explanation, no extra text).

1203

1204

1205 **Prompt for Navigation Tasks**

1206

1207 You are an expert pilot for an Autonomous Underwater Vehicle (AUV), designated as the
1208 "Control Expert". Your mission is to navigate a complex underwater environment to com-
1209 plete specific tasks. You will receive data from six cameras and location sensors. Your deci-
1210 sions must be precise, safe, and strategic.1211 **1. Tactical Briefing for the Area of Operations**1212 Before the mission begins, you must internalize the following intelligence about the op-
1213 erational area. This context is vital for interpreting sensor data and forming a macro-level
1214 strategy.

1215

1216

1217 **3. Mission Briefing and Sensor Data**1218 Task Description: **[Task Description]**1219 Target Object Name: **[Object Name]**1220 Target Object Reference Image: **[Object Image]**1221 Target Object Description: **[Object Description]**

1222

1223

1224 **5. Survey Navigation Commands**1225 Available Commands: 'ascend', 'descend', 'move left', 'move right', 'move forward', 'move
1226 backward', 'rotate left', 'rotate right', 'stop'.

1227 Command Execution: You must only issue ONE command per turn from the list above.

1228

1229

1230 **Remember:**1231 Conduct comprehensive reconnaissance! Systematic coverage = priority! Use efficient ex-
1232 ploration patterns! Catalog all special objects! Maintain exploration momentum! Always use
1233 format! Ignore all marine life! One continuous line between markers!

1234

1235

1236

1237 **Table 3: Performance of perception tasks across different prompts.**

1238

1239

1240

1241

Model	Shallow Water Environment (High Illumination)						Deep Water Environment (Low Illumination)					
	Multi-View Perception		Context-based Perception		Avg	Multi-View Perception		Context-based Perception		Avg		
	Vision	+Sonar	Vision	+Sonar		Vision	+Sonar	Vision	+Sonar			
GPT-4o-mini(prompt1)	34.55	34.55	20.00	33.33	30.61	14.55	20.00	3.33	6.67	11.14		
GPT-4o-mini(prompt2)	54.55	45.45	40.00	30.00	42.5	20.00	20.00	10.00	0.00	12.5		

1242
1243

A.6 THE IMPACT OF DIFFERENT PROMPTS ON PERCEPTION TASKS.

1244
1245
1246
1247

Due to the difficulty in finding a prompt that is suitable for all MLLMs, we test the impact of different prompts on the model. As shown in Table 3, we find that the impact was relatively small in deep water environment. Prompt1 is the prompt used in the main experiment, and prompt2 is the best prompt for GPT-4o-mini during the testing process.

1248
1249
1250
1251
1252
1253
1254
1255
1256
1257
1258
1259
1260
1261
1262
1263
1264
1265
1266
1267
1268
1269
1270
1271
1272
1273
1274
1275
1276
1277
1278
1279
1280
1281
1282
1283
1284
1285
1286
1287
1288
1289
1290
1291
1292
1293
1294
1295